https://doi.org/10.5194/amt-2019-359
Preprint. Discussion started: 14 October 2019

Atmospheric Measurement Techniques
Discussions

Airborne measurement of peroxy radicals using chemical amplification coupled with cavity ring down spectroscopy: the PeRCEAS instrument

[1]Midhun George, [1]Maria Dolores Andrés Hernández, [2]Vladyslav Nenakhov, [1]Yangzhuoran Liu, and [1]John Philip Burrows

[1] Institute of Environmental Physics, University of Bremen, Germany
[2] now at Flight Experiments, DLR Oberpfaffenhoffen, Germany

Correspondence to M. George (midhun@iup.physik.uni-bremen.de) and M.D. Andrés Hernández (lola@iup.physik.uni-bremen.de).

Abstract. Hydroperoxyl, HO_2, and organic peroxy, RO_2, radicals are reactive short lived species, which play a key role in tropospheric chemistry. Measurements of the sum of HO_2 and RO_2, known as RO_2^*, provide unique information about the chemical processing in an air mass. This paper describes the experimental features and capabilities of Peroxy Radical Chemical Enhancement and Absorption Spectrometer (PeRCEAS). This is an instrument designed for use on aircraft from the boundary layer to the lower stratosphere. PeRCEAS combines the amplified conversion of peroxy radicals to nitrogen dioxide, NO_2, with the sensitive detection of NO_2 using absorption spectroscopy (CRD) at 408 nm. PeRCEAS is a dual channel instrument, with two identical reactor-detector lines working out of phase with one another at a constant and defined pressure lower than ambient. The suitability of PeRCEAS for the airborne measurement in the free troposphere was evaluated by extensive characterisation and calibration under atmospherically representative conditions in the laboratory. The use of the alternating modes of the two instrumental channels captures successfully short term variations in the composition of RO_2^* in ambient air. For 60s measurement, the RO_2^* detection limit for a minimum (2σ) NO_2 detectable mixing ratio < 60 pptv, is < 2 pptv under controlled conditions in the range of atmospheric pressures and temperature gradients expected in the free troposphere. PeRCEAS has been successfully deployed in different airborne campaigns onboard the High Altitude LOng range research aircraft (HALO) for the study of the composition of the free troposphere within the missions OMO in 2015 and EMeRGe in 2017 and 2018.

1. Introduction

Hydroperoxyl, HO_2, and organic peroxy, RO_2, radicals, collectively known as RO_2^*, ($RO_2^* = HO_2 + \Sigma RO_2$; being R any organic chain) having an unpaired spin are highly reactive free radicals. They play important roles in the tropospheric chemistry. During the day, they are formed in the atmosphere following the oxidation of carbon monoxide, CO, and methane, CH_4, and many volatile organic compounds (VOCs). They participate in catalytic cycles, which produce and destroy ozone, O_3. Their temperate dependent reactions form temporary reservoirs (e.g. peroxynitrates like peroxyacetylnitrate, PAN, $CH_3CO.O_2.NO_2$), which are transported in the troposphere. In the presence of sufficient NO_x (Σ (nitrogen monoxide, NO, + nitrogen dioxide, NO_2)), the reaction of RO_2^* with NO forms NO_2 and hydroxyl radical, OH, which is the most important tropospheric oxidizing agent. The organic-oxy radical RO, which contain hydrogen atoms, often react with molecular oxygen, O_2, to form HO_2 and oxygenated volatile organic compounds, OVOC like aldehydes and ketones. The latter are oxidized by OH and photolysed to produce ultimately RO_2^*.

Overall the RO_2^* influence the amounts and distributions of OH and O_3 and thus the oxidising capacity of the troposphere. Consequently, knowledge about the spatial distribution and concentration of RO_2^* is essential to test our understanding of the tropospheric chemistry.

The RO_2^*concentrations and mixing ratios are small because of their high reactivity. Consequently the RO_2^* measurement requires sensitive and accurate techniques. With the exception of the freezing of air and subsequent use of the matrix isolation electron spin resonance technique (Mihelcic et al., 1985), there are no direct spectroscopic measurements of HO_2, RO_2 or RO_2^* in air. RO_2^* has been measured using the technique of chemical amplification (Cantrell and Stedman, 1982; Hastie et al., 1991). This approach converts by addition of NO and CO, HO_2 and those RO_2 to NO_2. The rate coefficients of the HO_2 and RO_2 reactions with NO are very similar. Larger RO_2, which do not react with NO to form NO_2, are not observed but are generally negligibly small compared to the amount of $RO_2^*$with HO_2 and CH_3O_2 in most conditions being the dominant peroxy radicals. The OH formed in the reaction cell reacts with CO to reform HO_2 in a chain reaction. Similarly, chemical amplification using a CO and SO_2 chain conversion in combination with chemical ionization mass spectrometry (CIMS) has been used for the measurement of RO_2^* [Reiner et al., 1997; Hanke et al., 2002]. In a further step, Edwards et al., [2003] and Hornbrook et al., [2011], reported about a PerCIMS instrument with two measurement modes, HO_2 and Σ RO_2, which are achieved by varying NO, SO_2 and O_2 concentrations in order to change relative sensitivities. Recently, the use of iodide and bromide as primary ions in CIMS for the measurement of HO_2 in laboratory measurements under controlled conditions has been reported [Sanchez et al., 2016; Albrecht et al., 2019]. Although still subject to interferences this technique seems to provide promising results. HO_2 has also been successfully measured by the conversion of HO_2 to OH, which is then measured by laser induced fluorescence, LIF, based on a technique known as Fluorescence Assay by Gas Expansion, FAGE, pioneered by Hard et al., [1984), and further modified by several scientific groups [Creasy et al., 1997; Kanaja et al., 1999; Holland et al., 2003, Faloona et al., 2004]. Potential spectral and chemical interferences have been largely investigated (Ren et al., 2004]. The interference of some RO_2 radicals into the HO_2 signal reported by Fuchs et al., [2010, 2011] can be minimised by controlling the NO concentration added for conversion into OH [Whalley et al., 2013; Lew et al., 2018].

In the last decades, ground based measurements of RO_2^* and HO_2 have been successfully made in a wide variety of environments [Monks et al, 1998, 2009 and references herein; Burkert et al., 2001 a and b; Carslaw et al., 2002, Fleming et al., 2006 a and b; Emmerson et al., 2007; Qui et al., 2007; Kanaja et al., 2007, 2012; Hofzumahaus et al., 2009; Andrés-Hernández et al., 2009; 2010, Mao et al., 2010, Kukui et al., 2014; Lelieveld et al., 2018]. The majority of measurements of RO_2^* or HO_2 were made in field campaigns on the boundary layer, which aimed at understanding the chemistry in the lower troposphere. These case studies have improved considerably our knowledge of the role of RO_2^* in tropospheric boundary layer chemistry. In contrast, the number of unequivocal measurements of peroxy radicals in the free troposphere is still quite limited. Mechanical and safety constraints as well as the temporal and special variability in the chemical composition of the air masses make the measurement in airborne platforms specially challenging. High instrumental accuracy, sensitivity and specificity are required to unequivocally determine potential spectral and chemical interferences [see Green et al., 2003, 2006; Zanis et al., 2003; Clemitshaw, 2004 and references herein; Heard 2006, and references herein, Stone et al., 2012 and references herein; Ren et al., 2012].

To meet these challenges, the PeRCEAS (Peroxy Radical Chemical Enhancement and Absorption Spectrometer) instrument was designed by the Institute of Environmental Physics of the University of Bremen (IUP-UB) for the airborne measurement of RO_2^* in the free troposphere and lower stratosphere for the deployment on board the HALO (High Altitude LOng range) research aircraft (www.halo.dlr.de).

PeRCEAS combines the **PeRCA** (Peroxyradical Chemical Amplification) and the **CRDS** (Cavity Ring Down Spectroscopy) techniques in a dual channel instrument for the determination of the total sum of peroxy radicals, RO_2^*. The principle of these well-known techniques and their application to the RO_2^* measurement have been described in detail in a previous work [Hortsjann et al., 2014]. As explained above briefly, in a PeRCA configuration, the probed RO_2^* are converted into an amplified amount of NO_2 by adding NO and CO in excess to the sampling air in the inlet. A modulated signal is obtained by alternating the position for the CO addition between the so called amplified or amplification and non-amplified or background modes, respectively favouring or suppressing the conversion of radicals into NO_2. The instrumental amplification factor, the so called effective chain length ($eCL = RO_2^*/\Delta NO_2$; being ΔNO_2 the NO_2 formed by the chemical amplification) depends on the terminating physical and chemical processes resulting in non-radical products, which vary according to the instrumental characteristics and the measurement conditions [Cantrell and Stedman, 1982; Cantrell et al., 1984, 1996; Hastie et al., 1991; Clemitshaw et al., 1997, Kartal et al., 2010].

In CRDS [O'Keefe and Deacon, 1988; Atkinson, 2003; Brown, 2003; Berden and Engel, 2010 and references herein], which is now a well-established spectroscopic measurements technique, a monochromatic light pulse is trapped inside a high finesse optical cavity and the time decay of the intensity is measured. The concentration of an absorber of interest can be calculated from the decay times of the light pulse to 1/eth of its initial value, the so called ring down time, for a resonator containing (τ) or not containing (τ_0) the absorber. In PeRCEAS the absorber of interest is the NO_2 obtained by the radical amplification.

The ambient RO_2^* concentrations measured by PeRCEAS are then retrieved from the difference in the ring down times of the background and amplification modes of operation, provided that τ_0 and the total scattering do not change substantially during two consecutive sampling modes:

$$\Delta\alpha = \alpha_2 - \alpha_1 = \frac{n}{c_o}\left(\frac{1}{\tau_2} - \frac{1}{\tau_1}\right) = \sigma_{NO_2}\,\Delta[NO_2] = \sigma_{NO_2}\,[RO_2^*] \times eCL \qquad \text{[Eq.1]}$$

where α_1, τ_1 , and α_2, τ_2 are respectively the absorption coefficients and ring down times for the background and amplification modes in the inlet, n is the refractive index of the medium, σ_{NO_2} is the absorption cross section of NO_2, and eCL is characteristic for each particular set up.

PERCA and absorption spectroscopy using high finesse optical cavities have been recently used for ground measurement of RO_2^*radicals [Liu et al., 2009; Wood and Charest, 2014; Chen et al., 2016]. PeRCEAS addresses the particular constrains related to the airborne measurement by improving the effective conversion of probed radicals in the reactor and the accuracy of the NO_2 measurement.

In this study the specifications and airborne performance of PeRCEAS are explained on a thorough description of laboratory characterisations and calibrations. The present work additionally uses the experience gained from the PeRCEAS deployment in three airborne measurement campaigns in the framework of the projects Oxidation Mechanism Observations, OMO, [see: www.mpic.de/ forschung/ kooperationen /halo/omo-mission.html;] and Effect of Megacities on the transport and transformation of pollutants on the Regional and Global scales, EMeRGe, [see: www.iup.uni-bremen.de/emerge/] onboard of the HALO platform.

2. PeRCEAS general description: mechanical and electrical setup

The core of the PeRCEAS airborne instrument is the DUALER inlet (DUal channel Airborne peroxy radical Chemical AmplifiER) installed inside a pylon and located in the outer part of the HALO fuselage, and two CRDS NO_2 detectors mounted in a rack inside the cabin. The first laboratory prototype reported by Hortsjann et al. [2014] has been significantly improved after deployment in various campaigns. The following description will essentially focus on the modified and optimised features of PeRCEAS.

The DUALER inlet (Figure 1) comprises two PeRCA chemical reactors with alternating measurement modes, which are out of phase with one another. The DUALER approach improves accuracy and resolution by enabling the continuous monitoring of both amplification and background signals. In order to minimise the impact of the changes in the ambient pressure during a flight on the chemical conversion, the DUALER pressure is stabilised in a pre-chamber prior to the addition of NO and CO. The DUALER outer geometry and weight are constrained by the aircraft pylon in use with the research aircraft HALO. However it was possible to modify the pre-chamber as compared to the initial prototype (from now on called DUALER I) to reduce wall contact at the inlet orifice, as well as the time required for mixing and pressure regulation. This optimised inlet configuration is called DUALER II in the text below.

The modifications in the PeRCEAS CRDS detectors for NO_2 targeted the signal stability and the in-flight adjustment of the optical alignment. The optical cavity remains similar to that described in Horstjann et al., [2014], i.e., a V-resonator of ca. 100 cm^3 volume, optimised to reduce the effect of vibration and temperature variations. As shown in figure 2, the current NO_2 detector houses a 100 mW continuous wave multimode diode laser (Stradus 405, wavelength ca. 408nm, max 100mW output power, Vortran Laser Technology Inc.), which simplifies and improves the fine adjustment of the laser and overcomes the necessity of using a piezo electric stack. The laser is aligned to the resonator using two motorised alignment mirrors [0.5'' aluminum mirrors mounted on Newport 8885 Picomotor Actuated Pint-Sized Center Mounts] which enable the correction of any mechanical displacement of the optical elements with respect to the resonator arising from misalignment due to vibration or mechanical shocks, during transport, installation or in-flight measurement. The beam profile can be continuously monitored by using a beam camera (BM-USB-SP907-OSI) to simplify the identification of misalignments or loss of performance of the optical system.

Concerning the data acquisition and processing, the current system is equipped with the latest National Instruments PXI-8840 computer with two PXI-6132 DAQ cards working with 1 M sample s^{-1} to measure the ring-down signal from both detectors and one PXI-6129 DAQ card working with 1 sample s^{-1} to measure all other sensor data like pressure, flow, temperature and humidity, etc.

Three identical interchangeable detectors (hereafter named Abbé: AB; Fraunhofer: FH; and Fresnel: FR) have been constructed and characterised for redundancy at the IUP-UB, of which two are always simultaneously deployed in measurement campaigns.

Additional components for the PeRCEAS operation like mass flow and pressure sensors/ controllers, gas cylinders and electronics are mounted in the main rack as described in Hortsjann et al, [2014]. The instrument rack in the aircraft cabin is connected to the DUALER through an aperture plate. Other ancillary parts of the PERCEAS, such as the vacuum pump, a secondary containment for dangerous gases (CO), a scrubber unit for NO_x/CO and the rest of gas cylinders are as also installed in the aircraft cabin (Figure 3).

3. PeRCEAS mode of operation

The mode of operation of PeRCEAS is optimised by systematically investigating the short and long term stability of the detector signal and the effect of potential interferences. Factors affecting the overall performance of PeRCEAS for airborne measurements are discussed in the following sections.

3.1. Measurement modes: integration time

Mode and modulation times are a compromise between the stability of the detector signal and the suitability of the sampling time for the chemical variability of the air probed.

Generally 650 to 800 ring-down times of the NO_2 absorption are averaged per second and individual ring-down times are exceptionally saved for sensitivity studies. Thus, the measurement of NO_2 is typically made at 1 Hz.

The optical stability of the NO_2 measurement with respect to non-systematic signal noise was investigated with the help of the Allan deviation for the measurement of a constant amount of NO_2 at 200 mbar and 23°C. As can be seen in figure 4, the best span of time for the three PeRCEAS detectors seem to be between 20 s and 30 s with a minimum (2σ) detectable mixing ratio < 60 pptv (3.153×10^8 molecules cm^{-3} at the measurement conditions). Slow temperature drifts over a longer averaging times impact on both the laser and the resonator characteristics.

Apart from the non-systematic noise, the stability of the detector response over the modulation time is decisive for the overall accuracy of the RO_2^* determination. As mentioned in the introduction, the ambient RO_2^* concentrations are calculated from the CRDS detector signals according to Eq. [1]. This requires the variation of τ_0 to be negligible over two consecutive modulation periods.

The effect of the τ variability in the accuracy and precision of the ΔNO_2 determination was investigated by a series of laboratory experiments focusing on the τ sensitivity to instabilities in the detector temperature. For this, different detector temperature gradients, ΔT, were applied to modulated signals generated by varying the sampled NO_2 concentration minutely under controlled laboratory conditions.

Figure 5 shows the effect of introducing temperature perturbations in the modulation signal between 11.5 and 12.1 ppbvNO_2. The ΔNO_2 determination with 1 min time resolution involves each background or amplification signal into the calculation of two consecutive ΔNO_2 values. As can be seen in the figure, a temperature perturbation affects both precision and accuracy of the retrieved ΔNO_2. For temperature gradients up to ΔT ~7°C h^{-1} the experimental precision of the ΔNO_2 determination remains within (2σ) 150 pptv (≈ 7.3×10^8 molecules cm^{-3} at the measurement conditions). For higher ΔT the retrieved ΔNO_2 deviates more significantly from the set value due to higher differences in τ within two consecutive modes. Applying running averages over two minutes improves the precision of the measurement.

According to the laboratory calibrations, a 60 s modulation cycle compromises optimally between the statistical significance and the noise of the signal. The first 20 s are removed to account for the short term pressure oscillations from switching modes and the transition time after switching. This cycle corresponds to 40 to 60 pptv NO_2 detection limits in the investigated detectors. Larger modulation times can lower the representativeness of the averages for ambient measurements in environments with large short term variability.

3.2. Sample flows and residence times

Sample and gas addition flows have different and related effects on the sensitivity of the PeRCEAS measurements. The rate of the sample flows determines the residence time in the reactor. This in turn impacts on the reaction time for the conversion of RO_2^* to NO_2, on the titration of ambient O_3, and on the thermal decomposition of peroxynitrates, and peroxynitric acid HO_2NO_2, which might produce an NO_2 interfering signal. Interferences are minimised by a rapid flow. Conversely, the RO_2^* to NO_2 conversion rate in the DUALER is determined by the concentration of the CO and NO addition gases. Laboratory tests show that CO is the most suitable gas to convert OH back to HO_2 in the chain reaction and that the eCL increases with the increase in CO added to the sample. However CO is a toxic and flammable gas with a lower explosive limit (LEL) of 12.5 in units of percentage by volume in air at room temperature and atmospheric pressure. This LEL is the minimum concentration necessary to support the gas combustion along with an ignition source such as a spark or flame [Zabetakis, 1965].

NO participates in both the chain carrier and chain termination reactions as explained in detail elsewhere [Hastie et al 1991, Mihele et al., 1999]. For a constant CO concentration, these reactions of NO determine the eCL at different pressures. The rate of titration of the sampled O_3 by NO to form NO_2 also depends on the concentration of NO added to the sample flow and the time for reaction before reaching the detector [Kartal et al., 2010].

In conclusion, the flows of the sampled ambient air and the added NO and CO in PeRCEAS are selected by compromising between safety regulations, limiting the amount and concentration of gases on board, and the eCL achieved for a particular residence time.

3.2.1. Effective chain length

The eCL of the DUALER reactors is determined in the laboratory by using a radical source. The latter uses water photolysis [Schultz et al., 1995]. A flow reactor providing a known amount of HO_2 or RO_2^* is placed inside a pressure chamber, having a vacuum sealed connection to the DUALER inlet. This setup is described in detail elsewhere [Kartal et al., 2009; Horstjann et al., 2014]. The photolysis of H_2O makes an OH and H, where the H reacts with O_2 in a three body reaction to make HO_2. The addition of CO is used to convert OH to HO_2. Alternatively, the addition of a hydrocarbon, RH, leads to the conversion in RO_2. For the HO_2 configuration, the HO_2 concentrations are calculated using

$$[HO_2] = \frac{\sigma_{H_2O}^{184.9nm}}{\sigma_{O_2}^{184.9nm}} \times \frac{[H_2O]}{[O_2]} \times [O_3] \qquad \text{[Eq.2]}$$

The value for the absorption cross section of H_2O at 184.9 nm, $\sigma_{H_2O}^{184.9nm} = (7.14 \pm 0.2) \text{ x } 10^{-20}$ cm^2 $molec^{-1}$ is taken from Cantrell et al., [1997] and Hofzumahaus et al., [1997], while the O_2 effective cross section $\sigma_{O_2eff}^{184.9nm}$ is determined experimentally for the particular calibration Hg lamp and the measurement conditions, according to Creasey et al. [2000] and Hofzumahaus et al. [1997].

Pure HO_2 and 1:1 HO_2: CH_3O_2 mixtures are generated at controlled pressures within expected airborne concentration ranges by adding 0.35% of CO or CH_4 respectively to the humidified air. Radical mixing ratios are changed every ten minutes and stepwise from 8 pptv to 150 pptv. The PeRCEAS eCL is determined as the slope of the measured NO_2 versus the set radical mixing ratios as exemplary shown in Figure 6 for 200mbar pressure and 30 ppmv addition of NO at the inlet.

In Figure 7 the PeRCEAS eCL = f ([NO]) obtained experimentally for inlet pressures between 200 and 350 mbar are depicted. As expected the eCL decreases with the NO concentration due to the terminating reactions forming HONO and CH_3ONO, the latter also causing the eCL being lower for the 1:1 HO_2:CH_3O_2 radical mixture. The experimentally determined eCL is higher for DUALER II, as expected from the reduction of radical losses in the pre-chamber respect to DUALER I. For a constant NO number concentration, the eCL increase with increasing pressure and is in good agreement with the results reported by Kartal et al., [2010].

A simple chemical box model was developed using the Kintecus software [Ianni, J. C, 2013; 2017; www.kintecus.com] to simulate the chemistry in the DUALER reactors. Dominant amplification and terminating reactions were included in the model as listed in Table 1. The model was initialised with 9% CO, 3 ppb O_3, 50 pptv HO_2 (6,07 x 10^8 molecule cm^{-3} at 500mbar) or a 50 pptv HO_2 + 50 pptv CH_3O_2 mixture. The value of k_{HONO} is the IUPAC preferred value [2017]. The k values for the radical wall losses are estimated from previous work [Kartal, 2009; Chrobry, 2013], and Mihele et al., [1999]. The rest of the rate constants used are taken from Burkholder et al, 2015.

The differences encountered between the experimental eCL and the model CL values are lower for DUALER II and are attributed to radical losses in the inlet pre-chamber. As previously reported by Kartal et al. [2010] radical losses in the pre-chamber might amount to ca. 50% of the ambient concentration. Figure 8 shows eCL versus CL for the DUALER II at 200 and 300mbar inlet pressure and different NO mixing ratios added to the inlet. The $CL_{modelled}/eCL_{measured}$ remains ~2 for HO_2 and ~1.5 for the 1:1 HO_2 and CH_3O_2 radical mixture. The present results confirm that the determination of the eCL in the laboratory for each particular setup and measurement condition is essential.

3.2.2. Titration of ambient O_3

The NO concentration added at the inlet has to be sufficient for a complete titration of the sampled O_3 within PeRCEAS before reaching the detector. Figure 9 depicts the O_3 decay simulated for 100 to 200 ppb ambient O_3, i.e., $5x10^{11}$ - $1.7x10^{12}$ molecules cm^{-3} at 200 and 300 mbar respectively, assuming the titration to be completed for a rest of [O_3] = $5x10^7$ molecules cm^{-3}. The O_3 absorption at 409 nm can be considered negligible. These results are in agreement with a series of laboratory measurements at 300 mbar for the DUALER II with a total flow of 500 ml min^{-1} as shown in Figure 10. The sample residence times for both DUALER systems are summarised in Table 2.

3.2.3. PAN and PPN thermal decomposition

Compounds like peroxy acetyl nitrate, PAN, or peroxypropionyl nitrate, PPN, alkylperoxynitrate and peroxynitric acid might decompose thermally inside PeRCEAS before the sample reaches the detector. This potentially leads to additional NO_2 and radical molecules, which are generally captured by both amplification and background modes i.e. cancelling and thus not interfering. However if the composition of the air mass varies at shorter time scales than the modulation time, the background and amplification signals will be differently affected and this can become an interfering source of radicals.

The production of peroxy radicals from the thermal decomposition of 1 ppb PAN at different expected flight temperatures was simulated by using a box model [Ianini, 2003] and the rate value reported by Atkinson et al. [2006]. As can be seen in figure 11, the production of radicals is also favoured at lower pressures. In a rapidly changing background the RO_2^* determination might be affected according to the temperatures and sample residence times in the DUALER (Table 2) but otherwise this source of radicals is considered to be negligible.

3.3. Operating pressure: radical losses and absolute humidity in DUALER

The PeRCEAS operating pressure is kept constant and below ambient pressure to preserve the radical chemical conversion in the inlet during the flight. However, the $\Delta P = P_{ambient} - P_{inlet}$ varies at different flight altitudes and leads to changes in the physical losses and the humidity in the pre-chamber. These may have a significant effect in the eCL, as reported by Kartal et al., [2010 and references herein].

To evaluate this effect for PeRCEAS, different ΔP were experimentally generated by changing the pressure in the pressure chamber while keeping inlet conditions like pressure, mixing ratios of the addition gases (NO, CO and N_2), sampling gas velocity (flow) and relative humidity invariable.

Figure 12 shows the variation of the eCL for 45ppm NO within a pressure range of $50\text{mbar} \le \Delta P \le 600\text{mbar}$. As can be seen in the figure, the eCL remains within 10% except for ΔP values < 100mbar. This might be the result of variations in the relative importance of terminating processes (wall losses versus chemical reactions) with the sample velocity through the pre-chamber [Kartal et al., 2010]. Consequently ΔP = 100 mbar is defined as the minimum operating pressure for PeRCEAS airborne measurements. This enables the measurement at flight altitudes up to 12 km.

Similarly, the effect of variations in the sampled air humidity on the eCL [Mihele and Hastie, 1998; Mihele et al., 1999] was investigated. In previous work, Reichert et al. [2003] confirmed the dependency of the eCL on the relative humidity for ground based measurements based on the similarity of the eCL values obtained for 20°C and 30°C at standard pressure, i.e., almost doubling the absolute water concentration. In the present experiment radical mixtures were sampled at 25°C changing the relative humidity between 1% and 25% which leads to a ca. 20 times increase the absolute $[H_2O]$. These conditions cover the $[H_2O]$ expected for a larger T range (-20 - 30°C) during airborne measurements in the free troposphere at 200mbar inlet pressures, as shown exemplary in figure 13 for real measurements on board of the HALO aircraft. The results in figure 14 for 45 ppm NO at 300mbar indicate that the PeRCEAS eCL remains invariable within the experimental error up to $[H_2O] \sim 1.4\times10^{17}$molec cm^{-3} and variations in the sample humidity does not lead to additional uncertainty in the RO_2^* retrieval.

4. PeRCEAS RO_2^* determination: Error calculation, detection limit and accuracy

The determination of RO_2^* concentrations from PeRCEAS measurements is subject to errors which a) intrinsically belong to the nature of the CRDS and PERCA techniques and can be characterised under controlled conditions in the laboratory, and b) result from the in-flight variability in the temperature, velocity and pressure conditions and cannot be easily reproduced in lab.

4.1. Errors related to the CRDS technique

Provided that the NO_2 absorption is the dominant process leading to light extinction at ~ 408 nm in the optical cavity of each detector, the absorption coefficient can be calculated from:

$$\alpha = \frac{n}{c_0}\left(\frac{1}{\tau_{sample}} - \frac{1}{\tau_0}\right) = \sigma_{NO_2} N \qquad \text{[Eq.3]}$$

where n is the refractive index of air, c_o is the speed of light in vacuum, τ_{sample} and τ_0 are the cavity ring down times with and without sample respectively, N is the number density of NO_2 in the sample and σ_{NO_2} is the absorption cross section of NO_2

which depends on the laser emission spectrum, the temperature and pressure (Vandaele et al., 1998, 2002). Under stable measurement conditions only σ_{NO_2}, τ and τ_0 might differ from one detector to another.

The **effective** σ_{NO_2} for each PeRCEAS NO_2 detector has been determined by using the convolution of the NO_2 absorption cross section from Vandele et al. [2002] on the normalised laser spectra from corresponding detector. The obtained values have been verified by regular sampling of NO_2 mixtures of known concentration in synthetic air.

The PeRCEAS lasers are kept at the maximum 100mW power to achieve the best Gaussian profile for the emission and are digitally modulated during operation. The laser emission spectrum is measured periodically in the laboratory by using a calibrated spectrometer (AvaSpec-ULS2048x64; 295-535 nm grating; 0.132 nm resolution) to verify the long term spectral stability. Figure 15 depicts exemplary a comparison of spectra obtained for the three PeRCEAS detectors with the high resolution NO_2 spectrum reported by Vandaele et al. [2002].

By integrating σ_{NO_2} under the normalized laser spectrum, the effective σ_{NO_2} are calculated to be 6.0 ± 0.3 x 10^{-19}, 6.3 ± 0.3 x $10^{-19}$and 6.4 ± 0.3 x 10^{-19} cm^2 $molecule^{-1}$ for the AB, FH and FR detectors respectively. The errors are calculated from the 2σ variation in the laser emission obtained from regular measurements and the error reported for the high resolution NO_2 spectra.

In addition, the effective σ_{NO_2} can be calculated by sampling known mixtures of NO_2 from commercial gas cylinders in synthetic air under controlled laboratory conditions, as shown in Figure 16.

According to Eq. [4], the effective NO_2 absorption cross-section is $1/c_0$ times the slope of the inverse of the measured τ versus the NO_2 number concentration:

$$\frac{1}{\tau_x} = c_0\sigma_{NO_2}[NO_2]_x + \frac{1}{\tau_0} \qquad \text{[Eq.4]}$$

The result of applying Eq. [4] to the PeRCEAS detectors at 200mbar is depicted in Figure 17. The obtained effective σ_{NO_2} agree within 5% with the values derived by integrating σ_{NO_2}under the normalized laser spectrum as described above.

The y intercept in figure 17 corresponds to $1/\tau_o$ values which are different for each detector. These variations are attributed to slight differences in the mirror reflectivity and in the overall alignment of the optical cavities. Under laboratory conditions □$_0$ is not expected to vary significantly for a particular detector.

4.2. Errors related to the PeRCA technique

The determination of RO_2^* mixing ratios from the ΔNO_2 measurement demands accurate knowledge of the eCL which depends upon physical parameters, such as temperature, pressure, wall losses, residence time in the reactor and the operating conditions as discussed in section 3. The main sources of uncertainty in the eCL determination are the radical generation, and the NO_2 determination from CRDS due to the accuracy of the σ_{NO_2}, which is calculated to be 5 % (2σ) (see 4.1).

In the current set up, the generation of peroxy radicals (Eq.2) has a precision < 3pptv (2σ). Based on the experimental reproducibility of radical calibrations the eCL precision is within 3 % under all conditions investigated. In addition to this experimental determination of the eCL has a 15 % uncertainty, dominated by the 10 % uncertainty of both $[O_3]$ and

$\sigma_{O_2 eff}^{184.9nm}$determinations using the calibration setup (Creasy et al., 2000; Kartal et al., 2009). The error associated with the determination of [H_2O] (0.05 %), [O_2] (0.5 %) and the $\sigma_{H_2O}^{184.9nm}$ value (1.4 %) are significantly lower.

Figure 18 shows the calculated eCL from 14 radical calibrations carried out over six months for 300 mbar pressure, ΔP = 200mbar, and 1 % relative humidity at the DUALER II inlet operating with 9 % CO and 45 ppmv NO addition for the amplification, by generating known concentrations of HO_2 and a (1:1) mixture of HO_2 and CH_3O_2 in synthetic air. For HO_2 the obtained eCL values are 36 ± 5 and 38 ± 5 for reactor 1 and reactor 2 respectively while 28 ± 4 and 29 ± 4 are obtained for the radical mixture. The error refers to the experimental precision (2σ) of the measurements.

4.3. Errors related to in-flight variability of background air: DUALER approach and RO_2^*retrieval

The in-flight dynamical stability of PeRCEAS is influenced by the stability of the sampling flows and pressures during the airborne measurement of RO_2^*. This stability depends on pressure variations experienced by the instrument when the aircraft is turning, ascending or descending, as well as in the presence of turbulence. The noise of the NO_2 signal is further enhanced by mechanical vibration and temperature variation. Though the in-flight temperature in the HALO cabin remains reasonably constant, during the instrumental preparation on the ground prior to the flight the cabin temperature might increase up to 40°C. This affects the stability of the ring down time signal and the accuracy of the reference measurements.

In addition to the above, the retrieval of the RO_2^* ambient mixing ratios requires a reliable discrimination of the interfering signals resulting from the variation of NO_2, O_3, PAN, PPN and any other molecules in the sampled air leading to additional absorption or scattering at ~408 nm. As mentioned before, background variations faster than two consecutive measurement modes might lead to erroneous radical determinations. In the case of aircraft measurements, this effect might be important due to the relative motion of the aircraft with respect to the air mass. The reliability of the PeRCEAS retrieval technique to effectively remove short term background variations was investigated in the laboratory by sampling HO_2 generated at a constant mixing ratio of 16 ± 2 pptv in synthetic air while varying O_3 up to 30 ppbv. The DUALER inlet was stabilised at 200 mbar and all other parameters like chamber pressure, mixing ratios of the addition gases (NO = 30 ppmv, CO = 9 % and N_2 =9 %), sampling flows (500 ml/min) and relative humidity (< 1 %) were controlled and kept constant.

As can be seen in Figure 19, the ΔNO_2 calculated from both detector signals remain around 700 pptv for a constant O_3 concentration, which is eCL times the HO_2 set value (i.e., ≈ 43 x 16 pptv). O_3 variations within one minute lead to opposite deviations from the 700 pptv value in the ΔNO_2 calculated from each system. This causes the HO_2 calculated from each system also to deviate in the same manner from the actual value. Because the two reactors are operated out of phase with one another, the final HO_2 data is the mean of the HO_2 determined by each detector from their respective ΔNO_2 using Eq.[1].

The ΔNO_2 calculated over 1 minute has a standard deviation in the order of the O_3 variation which leads to NO_2 through the NO titration in the reactor, as shown in the retrieved ΔNO_2 plot of figure 19. In the case of short term O_3 variations up to 30 ppbv, a 16 pptv HO_2 set mixing ratio (7.8×10^7 molecules cm^{-3} at 200 mbar and 25 °C) can be retrieved with a maximum deviation of 6 pptv (2.9×10^7 molecules cm^{-3} at 200 mbar and 25 °C) . The error in the retrieved HO_2 data results from the 15 % uncertainty of the eCL and the background NO_2 variation within one minute caused by the O_3 variations. This result is valid for all the background signal variations during a real-time measurement and proves the robustness of the DUALER approach for the retrieval of RO_2^* in a rapidly changing environment.

4.4. RO_2^* detection limit and accuracy

The PeRCEAS detection limit for RO_2^* ($LOD_{RO_2^*}$) is calculated by dividing the NO_2 detection limit (LOD_{NO_2}) by the corresponding eCL for each measurement condition set in the laboratory. Provided that $LOD_{NO_2}$is 60 pptv NO_2 (3.153×10^8 molecules cm^{-3}), 2σ over one minute as mentioned in section 3.1, the $LOD_{RO_2^*}$ varies between 1 and 2 pptv for the eCL values expected under dominant conditions in the free troposphere. The $LOD_{RO_2^*}$ can additionally be determined from the eCL calibration curves at different measurement conditions, according to:

$$LOD_{RO_2^*} = 3 \cdot S_a/m \qquad \text{[Eq.5]}$$

S_a is the standard deviation of the y-intercept and m is the slope of the NO_2 vs HO_2 calibration curve, (as in Fig 6, see 3.2.1.). For controlled laboratory conditions the $LOD_{RO_2^*}$ is 5.3×10^6 molecules cm^{-3} (≤ 2 pptv in all conditions investigated for DUALER I and DUALER II). As stated in 4.2., the accuracy is mainly dominated by the uncertainty in the eCL determination for each condition and amounts ~15 %.

Conversely, as stated in previous sections, the in-flight PeRCEAS detector signals are significantly affected by instabilities in physical parameters like pressure, temperature, flows, mechanical vibration and chemical composition which increase the uncertainty of the RO_2^* measurement. Therefore the in-flight error in the RO_2^* measurement is calculated by taking in to account the uncertainty of the eCL and the background variation in the signal within one modulation period as discussed in section 4.3.

Table 3 summarises the specifications of state of art instruments for the airborne measurement of peroxy radicals. Ground based instruments are also included for comparison.

As mentioned in the introduction, the Matrix Isolation and Electron Spin Resonance (MIESR) though being the only direct measurement technique of high precision, is not suitable for airborne measurements and of difficult implementation in field campaigns. Due to the differences in physical and chemical conditions used, a direct comparison between methods is challenging and only possible for time resolution and detection limit for a well-defined and controlled measurement conditions. The current sensitivity of PeRCEAS is competitive with other state of art instruments for the airborne measurement of peroxy radical.

The pressure regulation in PeRCA based airborne instruments results in lower eCL than ground based ones. The modulation time limits the resolution, except in the case of continuous measurement of background and amplification signal by different detectors (Liu et al 2014). The increase in resolution is however associated to uncertainties caused by differences in detectors accuracy. In addition to this, during ambient measurement the detection limit and uncertainty of PeRCA based instruments are strongly depending on the variation of O_3 and NO_2 in the sampled air mass. The speciation between HO_2 and $\sum RO_2$ is also difficult to achieve with this technique. LIF based instruments have a better detection limit but are subject to interferences from RO_2 in the sample.

5. PeRCEAS for airborne measurements of RO_2^*

PeRCEAS has up to date been successfully deployed and fully operational in 3 airborne measurement campaigns on board the HALO aircraft.

Figure 20 shows exemplary RO_2^* measured on the 25.08.2015 during the first flight deployment of PeRCEAS in OMO campaign. This particular mission flight aimed at probing the Asian monsoon outflow reaching the Arabian Peninsula, the outflow from Mount Etna and background air at flight altitudes above 12 km. RO_2^* measurements over Egypt from 5 to 8.5 km are shown in Figure 20 and 21. The ΔP ($\Delta P = P_{ambient} - P_{inlet}$) and $[H_2O]$ in the inlet remained below the calculated yield values to affect the eCL stability.

As can be seen in the figure, the effect of changes in inlet pressure during ascending and descending on the retrieved ΔNO_2 is not exactly identical in both detector signals. This leads to additional uncertainty in the RO_2^* determination when using the procedure discussed in section 4.3. For the data analysis, pressure spikes with 1 minute standard deviation higher than 2 mbar are flagged (P_Flag). In the measurement period shown the error in the retrieved RO_2^* remains around 20%.

Figure 22 shows the RO_2^* mixing ratios measured on the 11.07.2017 as example of the second flight deployment of PeRCEAS within the EMeRGe campaign in Europe. The pollution outflows of the Italian major population centers Po Valley and Rome were investigated. As can be seen in the figure RO_2^* reach up to 100 pptv along the track.

The first two hours of the flight are shown in more detailed on Figure 23 to illustrate the improvement in the dynamical stability achieved in successive airborne deployments. As can be seen in the figure, in the improved PeRCEAS the pressure fluctuations due to altitude changes and turbulence have been reduced up to 80% and the signal is not affected by altitude changes except for the maximum climbing rate directly after take-off. Furthermore, the beam camera and the motorised mirror mounts allow the identification and immediate correction of small misalignments. This improves significantly the instrumental performance while simplifying maintenance.

The results show the capability of PeRCEAS to capture RO_2^* variations even in rapidly changing air masses from the boundary layer to the upper troposphere. The instrument performance was stable over the 7 hours of mission flight indicating the robustness of the instrument towards mechanical vibrations and temperature variations. Further analysis of RO_2^* data together with models and other trace gas measurements are ongoing.

6. Summary and conclusion

The accurate measurement of peroxy radicals is essential for understanding the chemistry in the free troposphere. The PeRCEAS instrument has been designed, developed and thoroughly characterised for the measurement of the total sum of peroxy radicals onboard of airborne platforms. Parameters expected to affect the precision and accuracy of the measurement have been investigated in detail. Variations in the composition of the air mass within the modulation time are well captured when keeping the reactors out of phase and in alternating background/amplification modes with detectors of similar signal to noise ratio stability. Under controlled conditions in the laboratory the RO_2^* detection limit remains around 5.3×10^6 molecules cm^{-3} (≤ 2 pptv) over 60 s integration time for instrumental pressures from 160 to 350 mbar.

The performance of the PeRCEAS instrument has been proven to be suitable for measurements up to 12 km altitude during different airborne campaigns on board of HALO. The in-flight precision and detection limit depends critically on the features of the flight like pressure, temperature, flows, mechanical vibration, water number concentration and short term variations in the chemical composition, and must be calculated for each particular flight track. Therefore the optimisation of the instrument had a particular focus on the robustness of the dynamical and detector signal stabilities which makes PeRCEAS a reliable instrument for most flying conditions in the free troposphere.

Author contribution:

MG and MDAH designed the experiments, MG, VN, and YL carried out them. VN carried out the implementation in the HALO aircraft. MG prepared the manuscript with contributions from all co-authors. MDAH and JPB supervised the work.

Competing interests:

The authors declare that they have no conflict of interest.

Acknowledgements:

The authors acknowledge funding for this study by the University of Bremen, the state of Bremen, and the HALO SPP 1294 grant from the DFG Deutsche Forschungsgemeinschaft. Special thanks are to the mechanical workshop of the University of Bremen and to Wilke Thomssen for the support in the construction and certification of the PeRCEAS instrument. The authors also thank the colleagues of the OMO and EMeRGe communities for their collaboration, helpful discussions and support during campaigns.

References

Albrecht, S.R., Novelli, A., Hofzumahaus, A., Kang, S., Baker, Y., Mentle, T., Wahner, A., and H. Fuchs: Measurements of hydroxyperoxy radicals (HO_2) at atmospheric concentrations using bromide chemical ionisation mass spectrometry, Atmos. Meas. Tech., 12,981-902, https://doi.org/10.5194/amt-12-891-2019, 2019.

Anderson, D.C., Pavelec, J., Daube, C., Herndon, S.C., Knighton, W.B., Lerner, B.M., Roscioli, J.R., Yacovitch, T.I., and Wood, E.C.: Characterization of ozone production in San Antonio, Texas, using measurements of total peroxy radicals, Atmos. Chem. Phys., 19, 2845–2860, https://doi.org/10.5194/acp-19-2845-2019, 2019.

Andrés-Hernández, M.D., Kartal, D., Reichert, L., and Burrows, J.P., Meyer Arnek, J., Lichtenstern, M., Stock, P., Schlager, H.: Peroxy radical observations over West Africa AMMA 2006: Photochemical activity in the outflow of convective systems, ACP, 9, 3681-3695, 2009.

Andrés-Hernández, M. D., Stone, D., Brookes, D. M., Commane, R., Reeves, C. E., Huntrieser, H., Heard, D. E., Monks, P. S., Burrows, J. P., Schlager, H., Kartal, D., Evans, M. J., Floquet, C. F. A., Ingham, T., Methven, J., and Parker, A. E.: Peroxy radical partitioning during the AMMA radical intercomparison exercise, Atmos. Chem. Phys., 10, 10621-10638, doi :10.5194/acp-10-10621-2010, 2010.

Atkinson, D.B.: Solving chemical problems of environmental importance using cavity ring-down spectroscopy, Analyst, 128, 117–125, 2003.

Atkinson, R., Baulch, D. L., Cox, R. A., Crowley, J. N., Hampson, R. F., Hynes, R. G., Jenkin, M. E., Rossi, M. J., and Troe, J.: Atmos. Chem. Phys., 6, 3625, 2006; IUPAC Subcommittee for Gas Kinetic Data Evaluation, (http://iupac.pole-ether.fr).

Brown, S.: Absorption Spectroscopy in High-Finesse Cavities for Atmospheric Studies, Chem. Rev., 103, 5219−5238, 2003.

Burkert, J., Behmann, T., Andrés Hernández, M. D., Weissenmayer, M., Perner, D., and Burrows, J. P.: Measurements of peroxy radicals in a forested area in Portugal, Chemosphere, 3, 3327–3338, 2001a.

Burkert, J., Andrés Hernández, M. D., Stöbener, D., Burrows, J. P., Weissenmayer, M., and Kraus, A.: Peroxy radical and related trace gas measurement in the marine boundary layer above the Atlantic Ocean, J. Geophys. Res., 106, 5457–5477, 2001b.

Burkholder, J. B., Sander, S. P., Abbatt, J. ,Barker, J. R., Huie, R. E., Kolb, C. E., Kurylo, M. J., Orkin, V. L. Wilmouth, D. M., and P. H. Wine: Chemical Kinetics and Photochemical Data for Use in Atmospheric Studies,Evaluation No. 18, JPL Publication 15-10, Jet Propulsion Laboratory, Pasadena, 2015 http://jpldataeval.jpl.nasa.gov.

Cantrell, C. A. and Stedman, D. H.: A possible technique for the measurement of atmospheric peroxy radicals, Geophys. Res. Lett., 9, 846–849, 1982.

Cantrell, C. A., Stedman, D. H., and Wendel, G. J.: Measurement of atmospheric peroxy radicals by the chemical amplification, Anal. Chem., 56, 1496–1502, 1984

Cantrell, C.A., Shetter, R.E., Lind, A.J., McDaniel, A.H. and Calvert, J.G.: An improved chemical amplifier technique for peroxy radical measurements, J. Geophys. Res, 98, 2897-2909, 1993.Cantrell, C.A., Shetter, R.E., and Calvert, J.G., Dual-inlet chemical amplifier for atmospheric peroxy radical measurements, Analytical Chemistry, 68, 4194-4199, 1996.

Carslaw, N., Creasey, D.J., Heard, D.E., Jacobs, P.J., Lee, J.D., Lewis, A.C., Bauguitte, S., Penkett, S.A., Monks, P.S., Salisbury, G.: Eastern atlantic spring experiment 1997 (EASE97) 2. Comparisons of model concentrations of OH, HO_2, and RO_2 with measurements. Journal of Geophysical Research 107 (D14), 4190, doi:10.1029/2001JD001568, 2002.

Chen, Y., Chengqian, Y., Zhao, W., Fang, B., Xuezhe, X., Gai, Y., Lin, X., Chend, W., and Zhang, W.: Ultra-sensitive measurement of peroxy radicals by chemical amplification broadband cavity-enhanced spectroscopy, Analyst, 2016, 141, 5870, doi: 10.1039/c6an01038e, 2014.

Chrobry, A.: Development and laboratory characterization of a sampling system for airborne measurements of peroxy radicals using chemical amplification, Ph. D. dissertation, University of Bremen, Bremen, 2013.

Clemitshaw, K:C.; Carpenter, L.J., Penkett, S.A. and M.E. Jenkin: A calibrated peroxy radical chemical amplifier for ground-based tropospheric measurements, J. of Geophys. Res., Vol 102, D21, 25,405-25,416, 1997.

Clemitshaw, K.C.: A review of instrumentation and measurement techniques for ground-based and airborne field studies of gas-phase tropospheric chemistry, Critical Reviews in Environmental Science and technology, 34; 1-108, doi: 10.1080/10643380490265117, 2004.

Creasey, D.J., Heard, D.E., Halford-Maw, P.A., Pilling, M.J., Whitaker, B.J.: Implementation and initialdeployment of a field instrument for measurement of OH and HO_2 in the troposphere by laser-induced fluorescence, Journal of the Chemical Society, Faraday Transactions 93, 2907-2913, 1997.

Creasey, D., Heard, D. E., and Lee, J. D.: Absorption cross-section measurements of water vapour and oxygen at 185 nm. Implications for the calibration of field instruments to measure OH, HO_2 and RO_2 radicals, Geophys. Res. Lett., 27(11), 1651–1654, 2000.

Edwards, G. D., Cantrell, C. A., Stephens, S., Hill, B., Goyea, O., Shetter, R. E., Mauldin, R. L., Kosciuch, E., Tanner, D. J., and Eisele, F. L.: Chemical ionization mass spectrometer instrument for the measurement of tropospheric HO_2 and RO_2, Anal. Chem., 75, 5317–5327, https://doi.org/10.1021/ ac034402b, 2003.

Emmerson, K.M., Carslaw, N., Carlaw, D.C., Lee, J.D., McFiggans, G., Bloss, W.J., Gravestock, T., et al.: Free radical modelling studies during the UK TORCH Campaign in Summer 2003. Atmospheric Chemistry and Physics 7, 167–181. 2007.

Faloona, I.C., Tan, D., Lesher, R.L., Hazen., N., Frame, C.L., Simpas, J.B., harder, H., Martinez, M., Di Carlo, P., Ren, X ., and W.H. Brune: A Laser- induced Fluorescent Instrument for detecting Tropospheric OH and HO_2; Characteristics and Calibration, J. of Atmos. Chem. 47, 139-167, 2004.

Fleming, Z.L., Monks, P.S., Rickard, A.R., Bandy, B.J., Brough, N., Green, T.J., Reeves, C.E., Penkett, S.A.: Seasonal dependence of peroxy radical concentrations at a Northern hemisphere marine boundary layer site during summer and winter: evidence for radical activity in winter. Atmos. Chem. Phys. 6, 5415–5433. 2006a.

Fleming, Z.L., Monks, P.S., Rickard, A.R., Heard, D.E., Bloss, W.J., Seakins, P.W., Still, T.J., Sommariva, R., Pilling, M.J., Morgan, R., Green, T.J., Brough, N., Mills, G.P., Penkett, S.A., Lewis, A.C., Lee, J.D., Saiz-Lopez, A., Plane, J.M.C.: Peroxy radical chemistry and the control of ozone photochemistry at Mace Head, Ireland during the summer of 2002. Atmos. Chem. Phys. 6, 2193–221, 2006b.

Fuchs, H., Brauers, T., Häseler, R., Holland, Mihelcic, D., Müsgen, Rohrer, F., Wegener, R., and Hofzumahaus, A.: Intercomparison of peroxy radical measurements obtained at atmospheric conditions by laser-induced fluorescence and electron spin resonance spectroscopy, Atmos. Meas. Tech., 2, 55–64, www.atmos-meas-tech.net/2/55/2009/, 2009.

Fuchs, H., Brauers, T., Dorn, H.-P., Harder, H., Häseler, R., Hofzumahaus, A., Holland, F., Kanaya, Y., Kajii, Y., Kubistin, D., Lou, S., Martinez, M., Miyamoto, K., Nishida, S., Rudolf, M., Schlosser, E., Wahner, A., Yoshino, A., and Schurath, U.: Technical Note: Formal blind intercomparison of HO_2 measurements in the atmosphere simulation chamber SAPHIR during the HOxComp campaign, Atmos. Chem. Phys., 10, 12233–12250, https://doi.org/10.5194/acp-10-12233-2010, 2010.

Fuchs, H., Bohn, B., Hofzumahaus, A., Holland, F., Lu, K. D., Nehr, S., Rohrer, F., and Wahner, A.: Detection of HO_2 by laser-induced fluorescence: calibration and interferences from RO_2 radicals, Atmos. Meas. Tech., 4, 1209–1225, https://doi.org/10.5194/amt-4-1209-2011, 2011.

Green, T.J., Brough, N., Reeves, C.E., Edwards, G.D., Monks P.S., and Penkett, S.A.: Airborne measurements of peroxy radicals using the PERCA technique, J.Environ.Monitoring., 5, 75-83, 2002.

Green, T. J, Reeves, C.E., Fleming, Z.L, Brough, N., Rickard, R. A., Bandy, B.J, Monks, P.S.,and Penkett, S.A.: An improved dual channel PERCA instrument for atmospheric measurements of peroxy radicals, Journal of Environmental Monitoring, 8, 530–536, doi:10.1039/b514630e, 2006.

Hanke, M., Uecker, J., Reiner, T., and Arnold, F.: Atmospheric peroxy radicals: ROXMAS, a new mass-spectrometric methodology for speciated measurements of HO_2 and RO_2 and first results, Int. J. Mass Spectrom., 213, 91–99, https://doi.org/10.1016/S1387-3806(01)00548-6, 2002.

Hard, T. M., O'Brien, R. J., Chan, C. Y., and Mehrabzadeh, A. A.: Tropospheric free radical determination by FAGE, Environ. Sci. Technol.18, 768–777, 1984.

Hastie, D. R., Weissenmayer, M., Burrows, J. P., and Harris, G. W.: Calibrated chemical amplifier for atmospheric ROx measurements, Anal. Chem., 63, 2048–2057, 1991.

Heard, D.: Analytical Techniques for Atmospheric Measurement, Blackwell Publishing Ltd, Oxford, UK, 528 pp., doi:10.1002/9780470988510, 2006.

Hofzumahaus, A., Brauers, T., Aschmutat, U., Brandenburger, U.,Dorn, H. P., Hausmann, M., Heßling, M., Holland, F., PlassDulmer, C., Sedlacek, M., Weber, M., and Ehhalt, D. H.: Reply Geophys. Res. Lett., 24(23), 3039–3040, 1997.

Hofzumahaus, A., Rohrer, F., Lu, K., Bohn, B., Brauers, T., Chang, C.-C., Fuchs, H., Holland, F., Kita, K., Kondo, Y., Li, X., Lou, S., Shao, M., Zeng, L., Wahner, A., and Zhang, Y.: Amplified trace gas removal in the troposphere, Science, 324, 1702–1704, doi:10.1126/science.1164566, 2009.

Holland, F., Hofzumahaus, A., Schäfer, J., Kraus, A., and Pätz, H.-W.: Measurements of OH and HO_2 radical concentrations and photolysis frequencies during BERLIOZ, J. Geophys. Res.-Atmos., 108, 8246, https://doi.org/10.1029/2001jd001393, 2003.

Hornbrook, R. S., Crawford, J. H., Edwards, G. D., Goyea, O., Mauldin III, R. L., Olson, J. S., and Cantrell, C. A.: Measurements of tropospheric HO_2 and RO_2 by oxygen dilution modulation and chemical ionization mass spectrometry, Atmos. Meas. Tech., 4, 735–756, https://doi.org/10.5194/amt-4-735-2011, 2011.

Horstjann, M., Nenakhov, V., and Burrows, J.P.: Frequency stabilization of blue extended cavity diode lasers by external cavity optical feedback, Applied Physics B - Lasers & Optics. DOI: 10.1007/s00340-011-4705-y, 2011.

Horstjann, M., Andrés Hernández, M. D. , Nenakhov, V., Chrobry, A., and Burrows, J. P.: Peroxy radical detection for airborne atmospheric measurements using absorption spectroscopy of NO2, Atmos. Meas. Tech. 7, 1245-1257, doi: 10.5194/amt-7-1245-2014.

Ianni, J. C.: A Comparison of the Bader-Deuflhard and the Cash-Karp Runge-Kutta Integrators for the GRI-MECH 3.0 Model Based on the Chemical Kinetics Code Kintecus, pg.1368-1372, Computational Fluid and Solid Mechanics 2003, K.J. Bathe editor, Elsevier Science Ltd., Oxford, UK., 2003.

Ianni, James C., **Kintecus** , Windows Version 6.01, 2017, www.kintecus.com.

Kanaya, Y., Sadanaga, Y., Matsumoto, J., Sharma, U.K.,Hirokawa, J., Kajii, Y., Akimoto, H.: Nighttime observation of the HO_2 radical by an LIF based instrument on Oki island, Japan, and its possible origins. Geophys. Res. Lett., 26, 2179-2182, 1999.

Kanaya, Y., Cao, R., Akimoto, H. , Fukuda, M., Komazaki, Y. ,Yokouchi, Y. , Koike, M., Tanimoto, H., Takegawa, N.and Kondo, Y.: Urban photochemistry in central Tokyo: 1. Observed and modeled OH and HO_2 radical concentrations during the winter and summer of 2004, J. Geophys. Res., 112, D21312, doi:10.1029/2007JD008670, 2007.

Kanaya Y., Hofzumahaus, A., Dorn, H.-P., Brauers, T., Fuchs H., Holland, F., Rohrer, F., Bohn, B., et al.: Comparisons of observed and modeled OH and HO_2 concentrations during the ambient measurement period of the HO_xComp field campaign, Atmos. Chem. Phys., 12, 2567–2585, www.atmos-chem-phys.net/12/2567/2012/, doi:10.5194/acp-12-2567-2012, 2012.

Kartal, D.: Characterization and optimization optimisation of a dual channel PERCA for the investigation of the chemistry of peroxy radicals in the upper troposphere, PhD. thesis, University of Bremen, Germany, 2009.

Kartal, D., Andrés- Hernández, M.D., Reichert, L., Schlager H., and Burrows, J.P.: Technical Note: Characterisation of a DUALER instrument for the airborne measurement of peroxy radicals during AMMA 2006, ACP, 10, 3047-3062, doi: 10.5194/acp-1, 2010.

Kukui, A., Legrand, M., Preunkert, S., Frey, M. M., Loisil, R., Gil Roca, J., Jourdain, B., King, M. D., France, J. L., and Ancellet, G.: Measurements of OH and RO_2 radicals at Dome C, East Antarctica, Atmos. Chem. Phys., 14, 12373–12392, www.atmos-chem-phys.net/14/12373/2014/doi:10.5194/acp-14-12373-2014, 2014.

Lelieveld, J., Bourtsoukidids, E., Brühl, C., Fischer, H., Fuchs, H., Harder, H., Hofzumahaus, A, Holland, F., Marno, D., Neumeier, M., Pozzer, A., Schlager, H., Williams, J., Zahn, A., and Ziereis, H.: The South Asian monsoon—Pollution pump and purifier, Science, 10.1126/science.aar2501, 2018.

Lew, M. M., Dusanter, S., and Stevens, P. S.: Measurement of interferences associated with the detection of the hydroperoxy radical in the atmosphere using laser-induced fluorescence, Atmos. Meas. Tech., 11, 95–109, https://doi.org/10.5194/amt-11-95-2018, 2018.

Liu, Y., Morales-Cueto, R., Hargrove, J., Medina, D., and Zhang, J.: Measurements of peroxy radicals using chemical amplification cavity ringdown spectroscopy, Environ. Sci. Technol., 43, 7791–7796, 2009.

Liu, Y., and Zhang,: Atmospheric Peroxy Radical Measurements Using Dual-Channel Chemical Amplification Cavity Ringdown Spectroscopy, Anal. Chem., 86, 5391–5398, 2014.

Lopez, A., Plane, J.M.C.: Peroxy radical chemistry and the control of ozone photochemistry at Mace Head, Ireland during the summer of 2002. Atmospheric Chemistry and Physics 6, 2193–221, 2006.

Mao, J., Jacob, D. J., Evans, M. J., Olson, J. R., Ren, X., Brune, W. H., et al.: Chemistry of hydrogen oxide radicals (HOx) in the Arctic troposphere in spring, Atmos. Chem. Phys., 10, 5823–5838, www.atmos-chem-phys.net/10/5823/2010/doi:10.5194/acp-10-5823-2010, 2010.

Mihelcic, D., Müsgen, P., and Ehhalt, D. H.: An improved method of measuring tropospheric NO_2 and RO_2 by matrix isolation and electron spin resonance, J. Atmos. Chem., 3, 341–361, 1985.

Mihelcic, D., Holland, F., Hofzumahaus, A., Hoppe, L., Konrad, S., Müsgen, P., Pätz, H.-W., Schäfer, H.-J., Schmitz. T., Volz-Thomas, A., Bächmann, K., Schlomski, S., Platt, U., Gezer, A., Alicke, B., and Moortgat G.K.: Peroxy radicals during BERLIOZ at Pabstthum: Measurements, radical budgets and ozone production, J. Geophys. Res., 108, 8254, 2003.

Mihele, C.M., and Hastie, D.R.: The sensitivity of the radical amplifier to ambient water vapour. Geophys. Res. Letters, 25, 1911-1913, 1998.

Mihele, C.M., M. Mozurkewich, and Hastie, D.R.: Radical loss in a chain reaction of CO and NO in the presence of water: Implications for the radical amplifier and atmospheric chemistry, Intern. J. Chem. Kinetics, 31, 145-152, 1999.

Monks, P.S., Carpenter, L.J., Penkett, S.A., Ayers, G.P., Gillett, R.W., Galbally, I.E.,Meyer, C.P.: Fundamental ozone photochemistry in the remote marine boundary layer: the SOAPEX experiment, measurement and theory. Atmospheric Environment 32, 3647–3664, 1998.

Monks, P.S., Granier, C.; Fuzzi, S. et al.: Atmospheric composition change-global and regional air quality, Atmospheric Environment, 43, 5268–5350, doi:10.1016/j.atmosenv.2009.08.021, 2009.

Qi, B., Kanaya, Y. ,Takami, A., Hatakeyama, S. Kato, S., Sadanaga, Y., Tanimoto, H. and Kajii, Y.: Diurnal peroxy radical chemistry at a remote coastal site over the sea of Japan, J. Geophys. Res., 112, D17306, doi:10.1029/2006JD008236, 2007.

Reichert, L., Andrés Hernández, M.D., Stöbener, D., Burkert, J., and Burrows, J.P.: Investigation of the effect of water complexes in the determination of peroxy radical ambient concentrations: implications for the atmosphere, Journal of Geophys. Res, 108, D1, 4017- 4032, 2003.

Reiner, T., Hanke, M., and Arnold, F.: Atmospheric peroxy radical measurements by ion molecule reaction mass spectrometry: A novel analytical method using amplifying chemical conversion to sulfuric acid, J. Geophys. Res.-Atmos., 102, 1311–1326, https://doi.org/10.1029/96JD02963, 1997.

Ren, X., Mao, J., Brune, W.H., Cantrell, C.A., Mauldin III, R.L., Hornbrook, R.S., Koscluch, E., Olson, J.R., Crawford, J.H., Chen, G. and H.B. Singh: Airborne intercomparison of HOx measurements using laser-induced fluorescence and chemical ionization mass spectrometry during ARCTAS, Atmos. Meas. Tech., 5, 2025-2037, https://doi.org/10.5194/amt-5-2025-2012, 2012.

Sadanaga, Y., Matsumoto, J., Sakurai, K., Isozaki, R., Kato, S., Nomaguchi, T., Bandow, H., and Kajii, Y.: Development of a measurement system of peroxy radicals using a chemical amplification/laser-induced fluorescence technique, Rev. Sci. Instrum., 75, 864–872, https://doi.org/10.1063/1.1666985, 2004.

Sanchez, J., Tanner, D. J., Chen, D., Huey, L. G., and Ng, N. L.: A new technique for the direct detection of HO_2 radicals using bromide chemical ionization mass spectrometry (BrCIMS): initial characterization, Atmos. Meas. Tech., 9, 3851–3861, https://doi.org/10.5194/amt-9-3851-2016, 2016.

Schultz, M., Heitlinger, M., Mihelcic, D., and Volz-Thomas, A.: A calibration source for peroxy radicals with built-in actinometry using H2O and O2 photolysis at 185nm. J. Geophys. Res. 100, 18811-18816, 1995.

Stone, D., Whalley, L. K. and Dwayne E. Heard: Tropospheric OH and HO_2 radicals: field measurements and model comparisons, Critical Review, Chem. Soc. Rev., 41, 6348–6404, 2012.

Tan, Z., Fuchs, H., Lu, K., Hofzumahaus, A., Bohn, B. Broch, S. et al.; Radical chemistry at a rural site (Wangdu) in the North China Plain: observation and model calculations of OH, HO_2 and RO_2 radicals, Atmos. Chem. Phys., 17, 663–690, www.atmos-chem-phys.net/17/663/2017/doi:10.5194/acp-17-663-2017, 2017.

Vandaele, A. C., Hermans, C., Simon, P. C., Carleer, M., Colin, R., Fally, S., Merienne, M. F., Jenouvrier, A., and Coquart, B.: Measurements of the NO_2 absorption cross-section from 42 000 cm −1 to 10 000 cm −1 (238–1000 nm) at 220 K and 294 K, J. Quant. Spectrosc. Ra., 59, 171–184, 1998.

Vandaele, A. C., Hermans, C., Fally, S., Carleer, M., Colin, R., Mérienne, M.-F., Jenouvrier, A., and Coquart, B.: High resolution Fourier transform measurement of the NO_2 visible and near-infrared absorption cross-section: temperature and pressure effects, J. Geophys. Res., 107, 4348, doi:10.1029/2001JD000971, 2002.

Whalley, L. K., Blitz, M. A., Desservettaz, M., Seakins, P. W., and Heard, D. E.: Reporting the sensitivity of laser-induced fluorescence instruments used for HO_2 detection to an interference from RO_2 radicals and introducing a novel approach that enables HO_2 and certain RO_2 types to be selectively measured, Atmos. Meas.Tech., 6, 3425–3440, https://doi.org/10.5194/amt-6-3425-2013, 2013.

Wood, E. C., and Charest, J. R.: Chemical Amplification - Cavity Attenuated Phase Shift Spectroscopy Measurements of Atmospheric Peroxy Radicals Anal. Chem., 86, 10266–10273. 2014.

Wood, E. C., Deming, B.L. and Kundu, S.: Ethane-Based Chemical Amplification Measurement Technique for Atmospheric Peroxy Radicals Environ. Sci. Technol. Lett., 15-19, 2017.

Zabetakis, M. G.: Flanunability charactheristics of combustible gases and vapors. Washington U.S. Dept of the Interior, Bureau of Mines, Bulletin 627, 1965.

Zanis, P., Monks, P.S., Green, T.J., Schuepbach, E., Carpenter, L.J., Mills, G.P., Rickard, A.R. and Penkett, S.A.: Seasonal variation of peroxy radicals in the lower free troposphere based on observations from the FREE Tropospheric EXperiments in the Swiss Alps, Geophysical Research Letters . 30 (10), 1497, doi:10.1029/2003GL017122, 2003

Tables

Amplification reactions
$HO_2 + NO \rightarrow NO_2 + OH$
$CO + OH + M \rightarrow CO_2 + H + M$
$H + O_2 + M \rightarrow HO_2 + M$
$CH_3O_2 + NO \rightarrow CH_3O + NO_2$
$CH_3O + O_2 \rightarrow CH_2O + HO_2$
Terminating reactions
$OH + NO + M \rightarrow HONO + M$
$OH + NO_2 + M \rightarrow HNO_3 + M$
$CH_3O + NO + M \rightarrow CH_3ONO + M$
$OH + HO_2 \rightarrow H_2O + O_2$
$HO_2 + CH_3O_2 \rightarrow CH_3OOH + O_2$
$OH + OH + M \rightarrow H_2O_2 + M$
$OH + HONO \rightarrow H_2O + NO_2$
$OH + H_2O_2 \rightarrow HO_2 + H_2O$
$HO_2 + HO_2 \rightarrow H_2O_2 + O_2$
$HO_2 + NO_2 + M \rightarrow HO_2NO_2 + M$
$HO_2NO_2 + M \rightarrow HO_2 + NO_2 + M$
HO_2 (g) → HO_2 (s); k_{wall} = 1,4 s^{-1} CH_3O_2 (g) → CH_3O_2 (s); k_{wall}= 0,4 s^{-1}
O_3 reaction
$O_3 + NO \rightarrow O_2 + NO_2$

Table 1: Reactions used in a box model for the CL simulation of the PeRCEAS reactors.

P inlet	To DUALER I second addition point (s)			To detector (s)		
(mbar)	300 ml/min	500 ml/min	1000 ml/min	300 ml/min	500 ml/min	1000 ml/min
300	6.55	3.93	1.96	7.82	4.69	2.35
200	4.36	2.62	1.31	5.21	3.13	1.56
160	3.49	2.10	1.05	4.17	2.50	1.25
100	2.18	1.31	0.65	2.61	1.56	0.78
80	1.75	1.05	0.52	2.09	1.25	0.63
50	1.09	0.65	0.33	1.30	0.78	0.39
	To DUALER II second addition point (s)			To detector (s)		
300	7.73	4.64	2.32	13.18	7.91	3.95
200	5.15	3.09	1.55	8.79	5.27	2.64
160	4.12	2.47	1.24	7.03	4.22	2.11
100	2.58	1.55	0.77	4.39	2.64	1.32
80	2.06	1.24	0.62	3.51	2.11	1.05
50	1.29	0.77	0.39	2.20	1.32	0.66

Table 2: Sample residence times in PeRCEAS for different operating total flows and pressures. Inner volumes up to the detector increased from 132 cm^3 in DUALER I to 220 cm^3 in DUALER II.

Author	Year	Technique	eCL	LOD_{NO_2} (pptv)	$\mathrm{LOD}_{\mathrm{RO}_2^*}$ (pptv)	Averaging time (s)	Pressure (mbar)
Airborne instruments							
Green et al.	2002	PeRCA + Luminol	277 - 322 (3 ppmv NO + 7 % CO)	180	1	20	not controlled (from ground level to 7 km)
Kartal et al.	2010	PeRCA + Luminol	45 ± 7 (3 ppmv NO + 7.4 % CO)	130 ± 5	3 ± 2	60	200
Horstjan et al.	2014	PeRCA + OF-CEAS	110 ± 21 (6 ppmv NO + 9 % CO)	300	3 - 5	120	300
			55 ± 10 (6 ppmv NO + 9 % CO)	300	6	120	200
Hornbrook et al.	2011	PeRCIMS			2		200
Ren at al.	2012	LIF			0.1 (2σ)	60	up to 300
		PerCIMS			1 (2σ)	15	up to 300
This work		PeRCA + CRDS	62 ± 9 (30 ppmv NO 9 % CO)	60	< 2	60	200 to 350
Ground based instruments							
Cantrell et al.	1984	PeRCA + Luminol	1010 (3 ppmv NO + 10 % CO)		0.6	300	1000
Hastie et al.	1991	PeRCA + Luminol	120 (2 ppmv NO + 4 % CO)	50	2	10	1000
Cantrell et al.	1993	PeRCA + Liminol	300 (3 ppmv NO + 10 % CO)		< 2	60	1000
Reiner et.al.	1997	PeRCA + IMR-MS	100		10^6 molec. cm^{-3}		1000
Sadanaga et al	2004	PeRCA + LIF	190 (3 ppmv NO + 10 % CO)	61	2.7 (50 % RH) 3.6 (80 % RH)	60	1000
Liu et al.	2009	PERCA +	150 ± 50 (2σ)	150	10 (3σ)	60	1000

		CRDS		(3σ 10s)			
Wood et al.	2014	PeRCA + CAPS	168 ± 20 (3.75 ppmv NO 9.8 % CO)	12 (1σ 30s)	0.6 (40 % RH)	60	1000
Liu et al.	2014	PeRCA + CRDS	190		4	10	1000
Chen et al.	2016	PeRCA + IBBCEAS	91 ± 11 (7.7 ppmv NO 8.5 % CO)	49 and 62 for differen chanels	0.9 (10 % RH)	60	1000
Wood et al.	2017	ECHAMP + CAPS	25 (dry) and 17(50 % RH) (1 ppmv NO 2.3 % C_2H_6)	10 (1σ 45s)	1.6 (50 % RH)	90	1000
Anderson et al.	2019	ECHAMP + CAPS	23 (dry) and 12(58 % RH) (0.9 ppmv NO 1.3 % C_2H_6)	10 (1σ 45s)	1.6 (50 % RH)	120	1000
Edwards et al.	2003	PeRCIMS			0.4	15	1000
Fush et al.	2008	LIF			0.1	60	1000
Mihelcic et al.	2003	MIESR			2	1800	1000

Table 3: State of art instruments for the airborne measurement of peroxy radicals. Instruments for the ground based measurement are also included for comparison.

Figure captions

Figure 1: a) DUALER inlet, b) DUALER inside the pylon, c) DUALER installed in the fuselage of HALO

Figure 2: Top down view of the PeRCEAS NO_2 detector. On the left is a detail of the entrance of the optical cavity with picomotors for mirror adjustment. The laser beam is highlighted for clarification. On the right the laser beam exiting the cavity is additionally depicted.

Figure 3: PeRCEAS as installed on board of HALO for the OMO mission.

Figure 4: Allan variation for 5.6 ppbv of NO_2 at 200 mbar and 23 °C sampled by the PeRCEAS cavities: AB, FH, and FR.

Figure 5: Effect of variations in the resonator temperature on τ and ΔNO_2 accuracy. The mixing ratio of NO_2 is held constant; the depicted error bars correspond to the total uncertainty of the retrieved ΔNO_2. The first 20 s of each signal after a change in the set NO_2 mixing ratio are discarded to ensure the stability of the mixing ratio sampled.

Figure 6: PeRCEAS eCL determination for HO_2 at 200 mbar pressure and 30 ppmv NO added to the sample flow at the DUALER II inlet.

Figure 7: Variation of eCL with NO under laboratory conditions for DUALER I and DUALER II. The radical source is kept at 500mbar while the inlet pressure varies between 200 and 350 mbar.

Figure 8: PeRCEAS eCL versus CL at different conditions. Values for 200 mbar inlet pressures are filled dots (HO_2) and triangles (1:1 radical mixture). Non filled symbols are for 300 mbar inlet pressure. The CL has been modelled by using Kintecus [Ianni, 2003]. The 1:2 line is depicted for visual support.

Figure 9: Time resolution of the O_3 titration at 200 and 300 mbar corresponding to 100 and 200 ppbv O_3 as simulated from $O_3 + NO \rightarrow O_2 + NO_2$; k= 1,90 x 10^{-14} cm^3 $molec^{-1}$ s^{-1}.

Figure 10: PeRCEAS measurement of O_3 mixing ratios up to 100 ppbv for different [NO] in the addition gas using DUALER II. For clarity NO is scaled in ppmv and molecules cm^{-3}. The titration is completed when $NO_{2\ measured}$ / $O_{3\ set}$ reaches unity. The values obtained by each PeRCEAS reactor (R1 and R2) are depicted in different colours.

Figure 11: Box model simulation of the CH_3O_2 radical production from the thermal decomposition of 1 ppbv PAN at different temperatures and pressure.

Figure 12: Dependency of eCL on ΔP ($\Delta P = P_{ambient} - P_{inlet}$) as determined for PeRCEAS under controlled laboratory conditions for 45 ppmv NO and 300 mbar inlet pressure. The error bars represent the 1σ deviation of identical calibrations at each ΔP.

Figure 13: Example of vertical [H_2O] distribution measured by BAHAMAS on board HALO in July 2017 during the EMeRGe campaign in Europe. The humidity measured inside the DUALER is plotted in red for comparison.

Figure 14: Dependency of PeRCEAS eCL on inlet humidity at constant sampling flow, inlet pressure, ΔP, [NO], [CO] and [N_2].

Figure 15: Emission spectrum of the lasers used by PeRCEAS. The high resolution σ_{NO_2} at 294 K from Vandaele et al (2002) is also depicted for comparison.

https://doi.org/10.5194/amt-2019-359
Preprint. Discussion started: 14 October 2019

Figure 16: PeRCEAS measurement of known NO_2 mixing ratios in synthetic air (Airliquid 9.89 ± 0.2 ppmv NO_2 in SA) using the FH detector at 200 mbar and 500 ml/min sample flow.

Figure 17: Effective absorption cross section, σ_{NO_2}, obtained from NO_2 calibrations carried out at 200 mbar detector pressure for the PeRCEAS detectors: AB (red), FH (blue) and FR (green). Linear fits are also depicted for clarification.

Figure 18: Experimental eCL determination of the DUALER II reactors from a series of 14 calibrations with generated mixing ratios of HO_2 (in blue) and a (1:1) HO_2: CH_3O_2 radical mixture (in red) at 300 mbar inlet pressure, 200 mbar ΔP and 45 ppmv added NO at the inlet.

Figure 19: HO_2 retrieval while controlled changing O_3 background concentration under laboratory conditions using DUALER I. The blue shaded area shows the HO_2 produced in the source considering the 15 % uncertainty (2σ).

Figure 20: RO_2^* PeRCEAS airborne measurement during the OMO flight on 25.08.2015 at 160 mbar inlet pressure and with 15 ppmv NO added to the sample flow at the inlet.

Figure 21: RO_2^* PeRCEAS measurements during the OMO flight on 25.08.2015 along the flight track.

Figure 22: RO_2^* measurement along the flight track on 11.07.2017 during EMeRGe in Europe.

Figure 23: Detail of PeRCEAS airborne measurement during the EMeRGe flight on 11.07.2017 at 200 mbar inlet pressure and with 30 ppmv NO added to the sample flow at the inlet.

https://doi.org/10.5194/amt-2019-359
Preprint. Discussion started: 14 October 2019

Figures

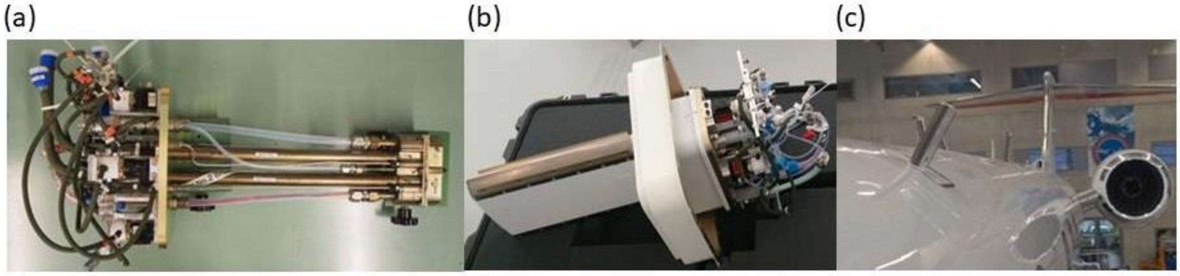

Figure 1: a) DUALER inlet, b) DUALER inside the pylon, c) DUALER installed in the fuselage of HALO.

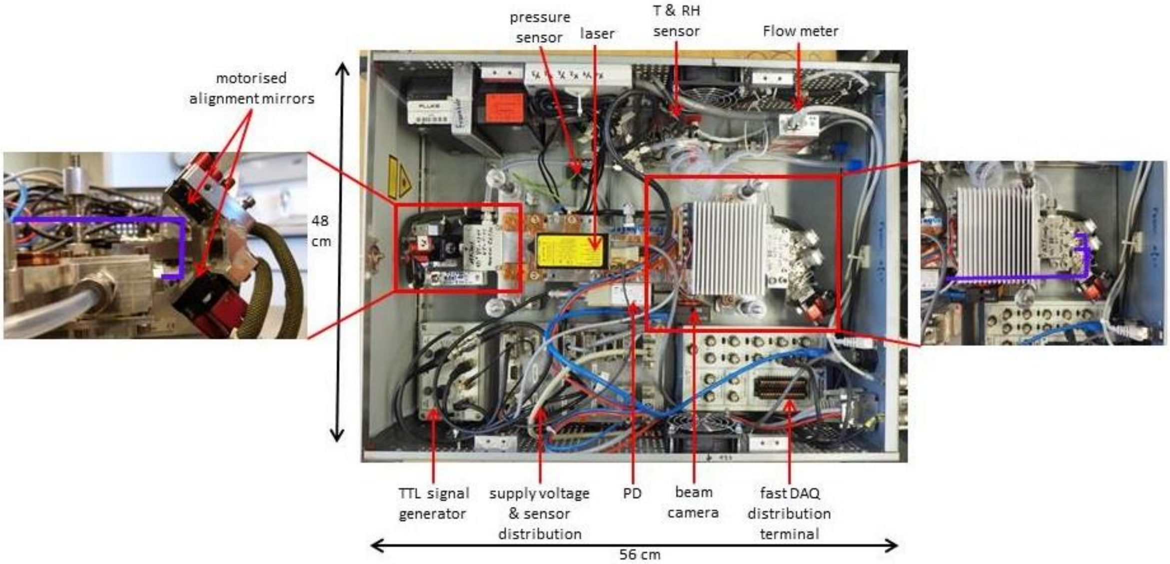

Figure 2: Top down view of the PeRCEAS NO_2 detector. On the left is a detail of the entrance of the optical cavity with picomotors for mirror adjustment. The laser beam is highlighted for clarification. On the right the laser beam exiting the cavity is additionally depicted.

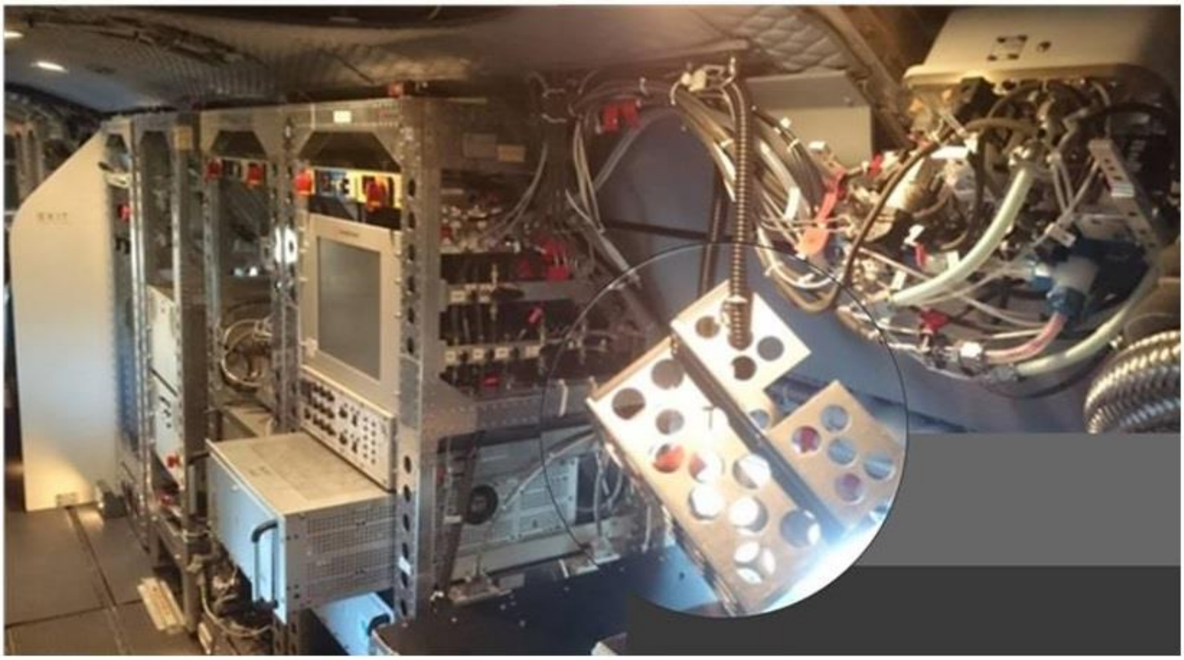

Figure 3: PeRCEAS as installed on board of HALO for the OMO mission.

https://doi.org/10.5194/amt-2019-359
Preprint. Discussion started: 14 October 2019

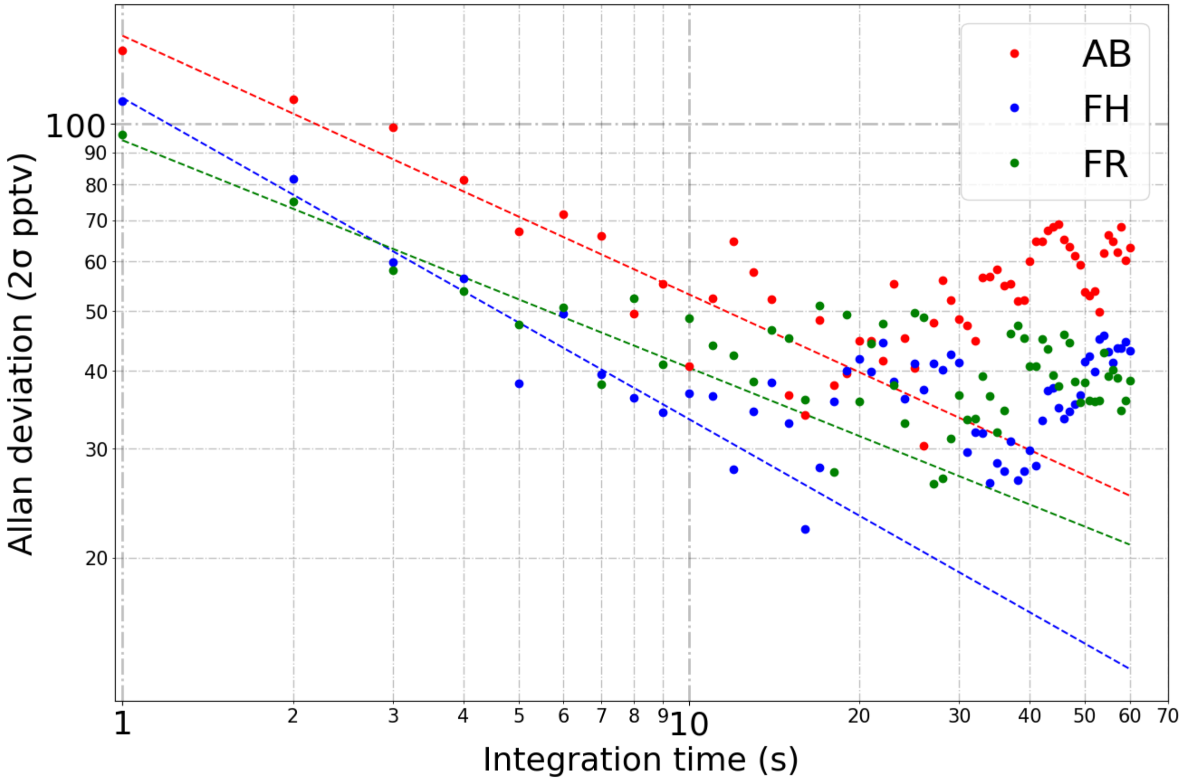

Figure 4: Allan variation for 5.6 ppbv of NO_2 at 200 mbar and 23 °C sampled by the PeRCEAS cavities: AB, FH, and FR.

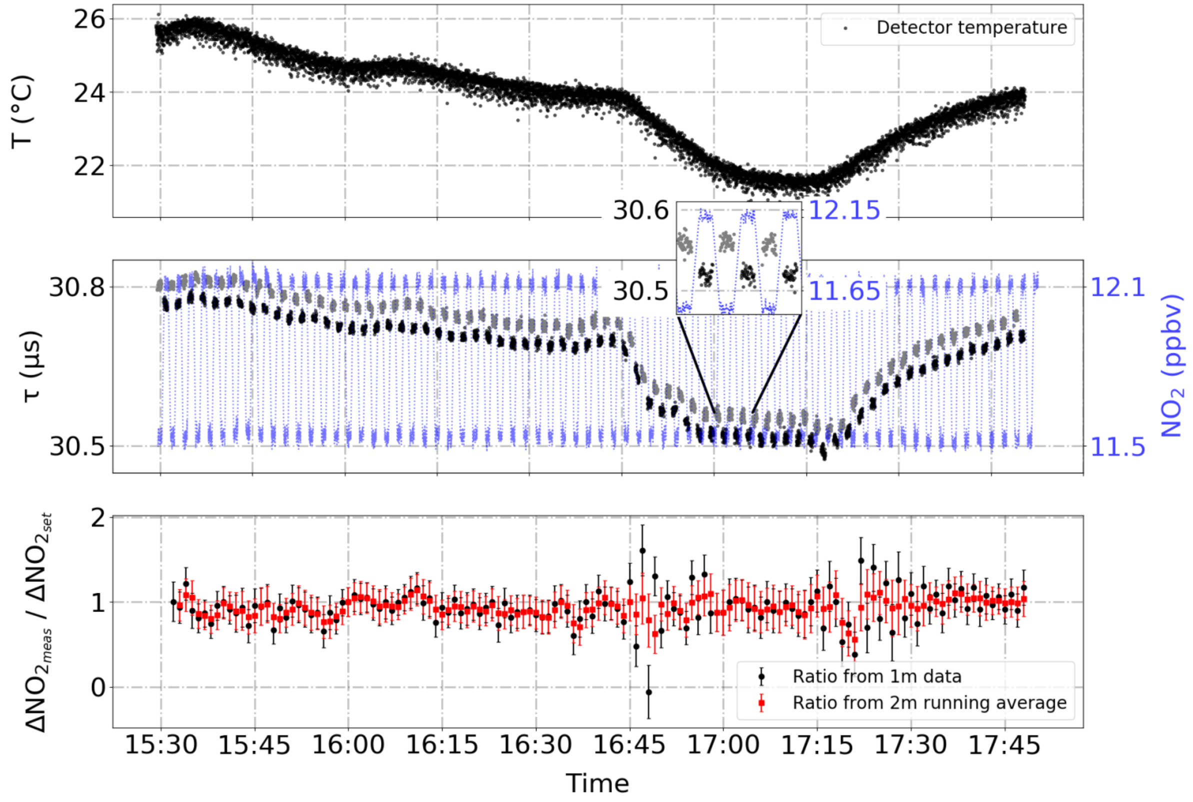

Figure 5: Effect of variations in the resonator temperature on τ and ΔNO$_2$ accuracy. The mixing ratio of NO$_2$ is held constant; the depicted error bars correspond to the total uncertainty of the retrieved ΔNO$_2$. The first 20 s of each signal after a change in the set NO$_2$ mixing ratio are discarded to ensure the stability of the mixing ratio sampled.

https://doi.org/10.5194/amt-2019-359
Preprint. Discussion started: 14 October 2019

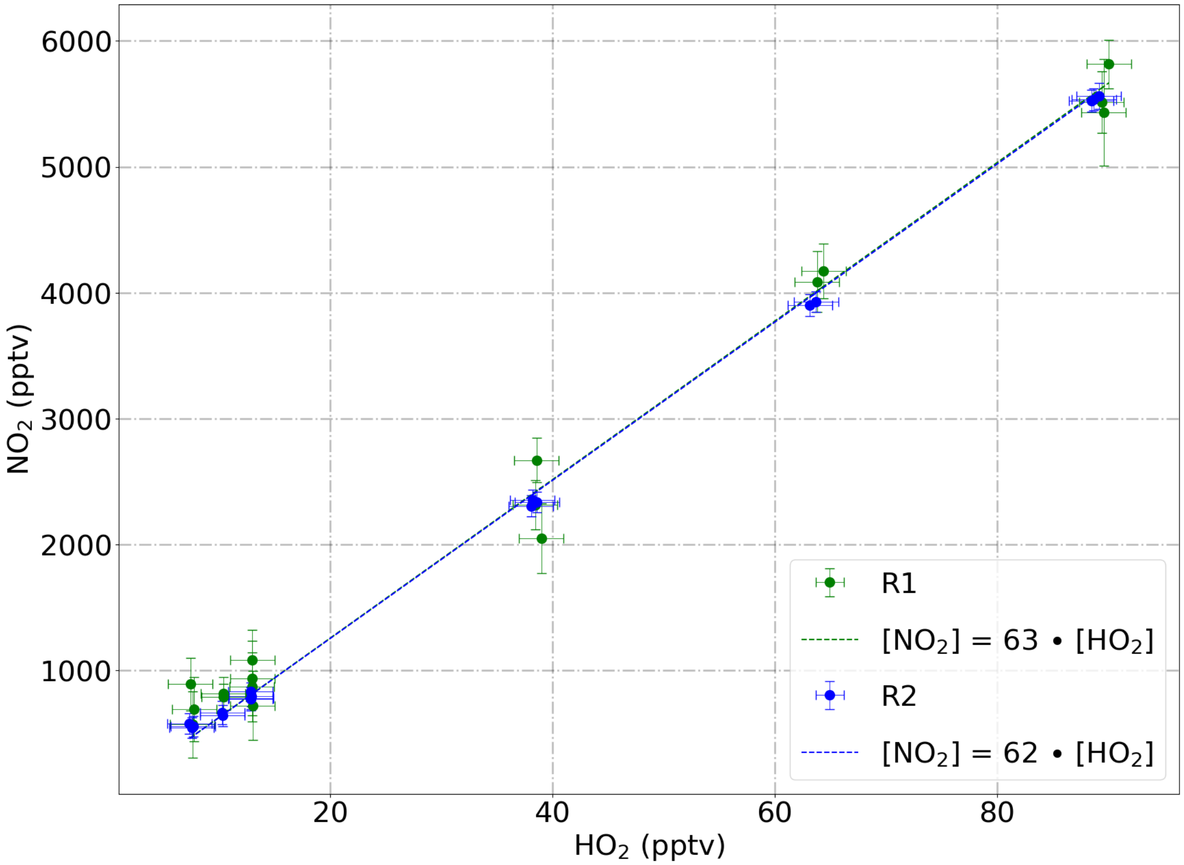

Figure 6: PeRCEAS eCL determination for HO_2 at 200 mbar pressure and 30 ppmv NO added to the sample flow at the DUALER II inlet.

https://doi.org/10.5194/amt-2019-359
Preprint. Discussion started: 14 October 2019

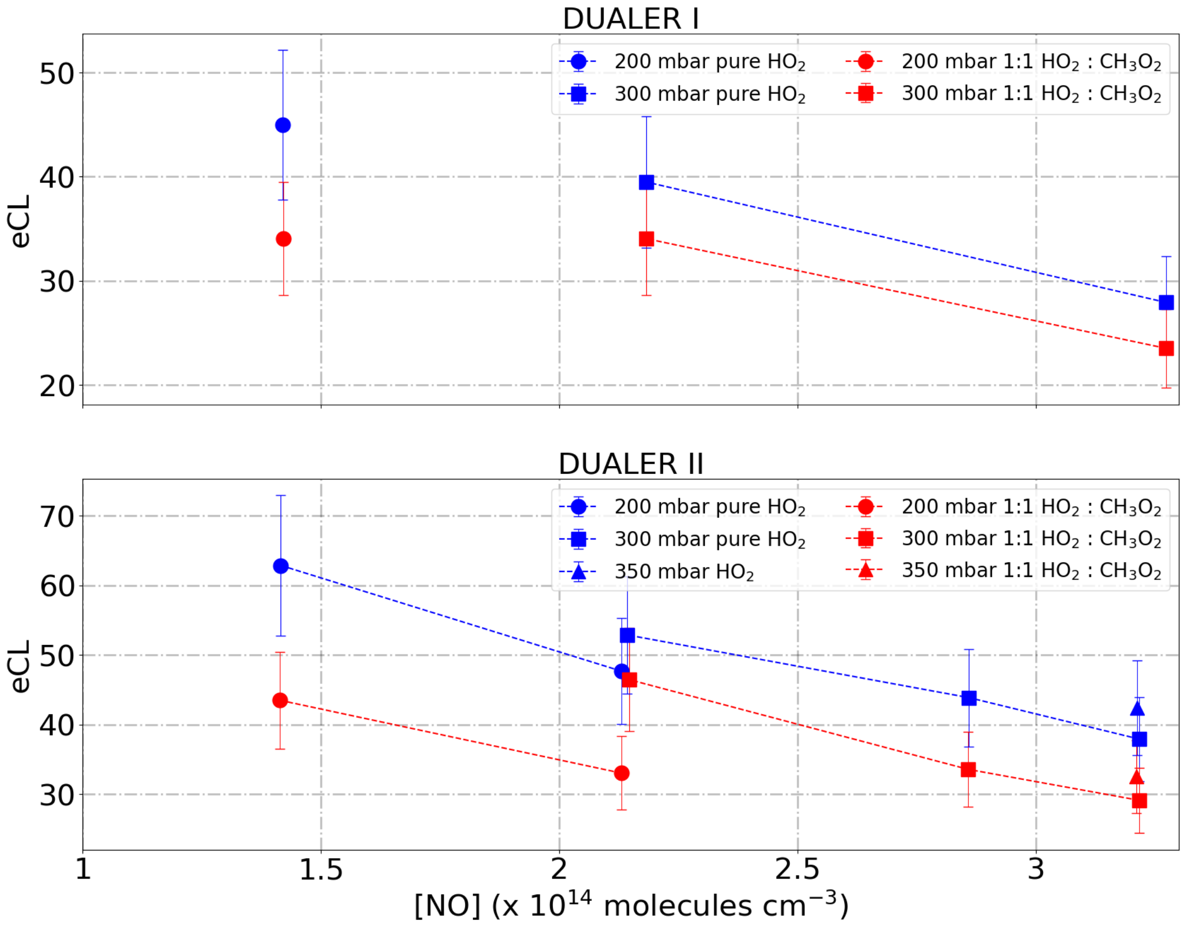

Figure 7: Variation of eCL with NO under laboratory conditions for DUALER I and DUALER II. The radical source is kept at 500mbar while the inlet pressure varies between 200 and 350 mbar.

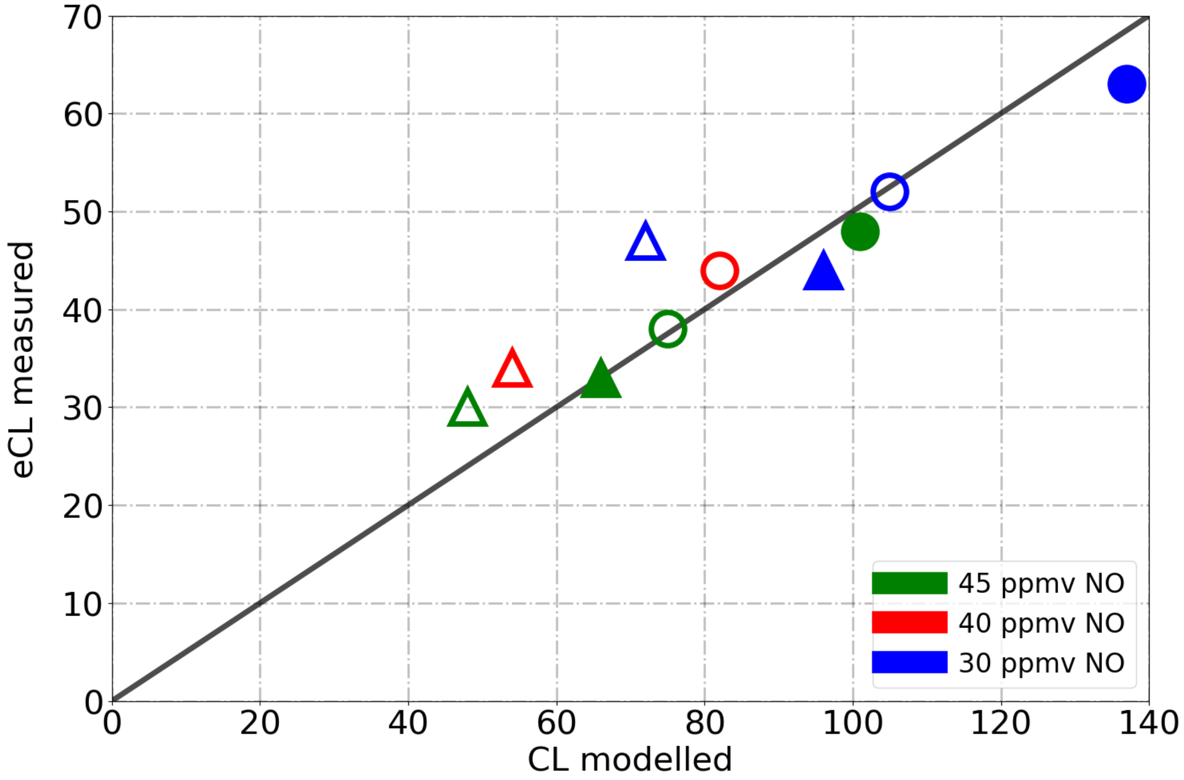

Figure 8: PeRCEAS eCL versus CL at different conditions. Values for 200 mbar inlet pressures are filled dots (HO_2) and triangles (1:1 radical mixture). Non filled symbols are for 300 mbar inlet pressure. The CL has been modelled by using Kintecus [Ianni, 2003]. The 1:2 line is depicted for visual support.

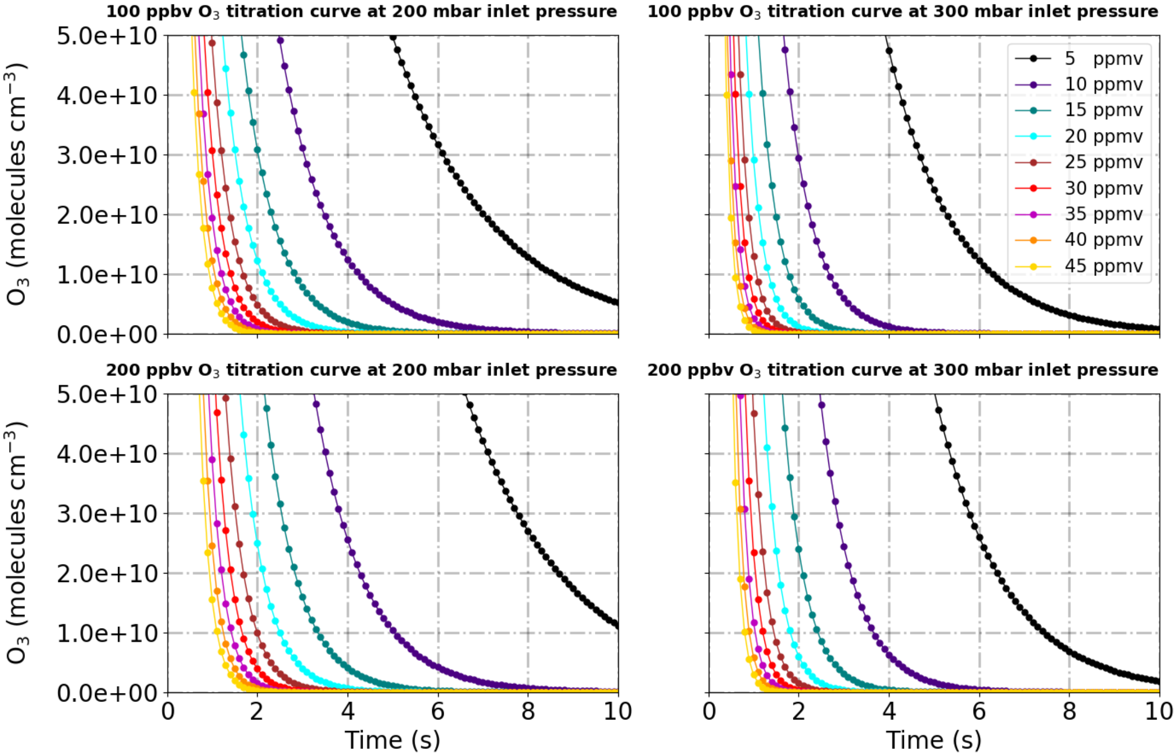

Figure 9: Time resolution of the O_3 titration at 200 and 300 mbar corresponding to 100 and 200 ppbv O_3 as simulated from $O_3 + NO \rightarrow O_2 + NO_2$; k= 1,90 x 10^{-14} cm^3 $molec^{-1}$ s^{-1}.

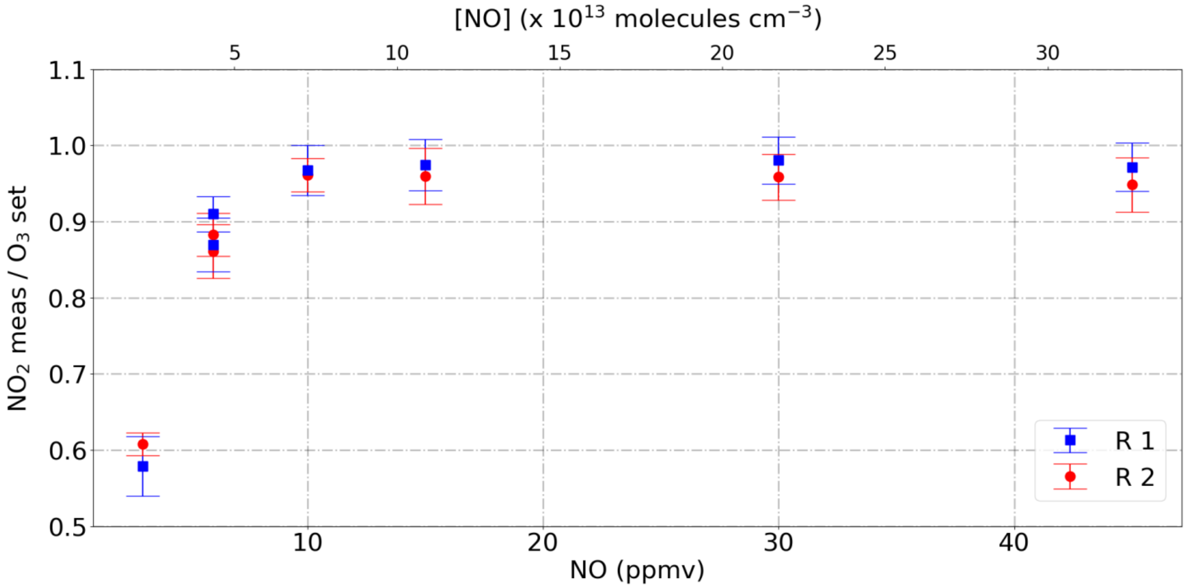

Figure 10: PeRCEAS measurement of O_3 mixing ratios up to 100 ppbv for different [NO] in the addition gas using DUALER II. For clarity NO is scaled in ppmv and molecules cm^{-3}. The titration is completed when $NO_{2\ measured}$ / $O_{3\ set}$ reaches unity. The values obtained by each PeRCEAS reactor (R1 and R2) are depicted in different colours.

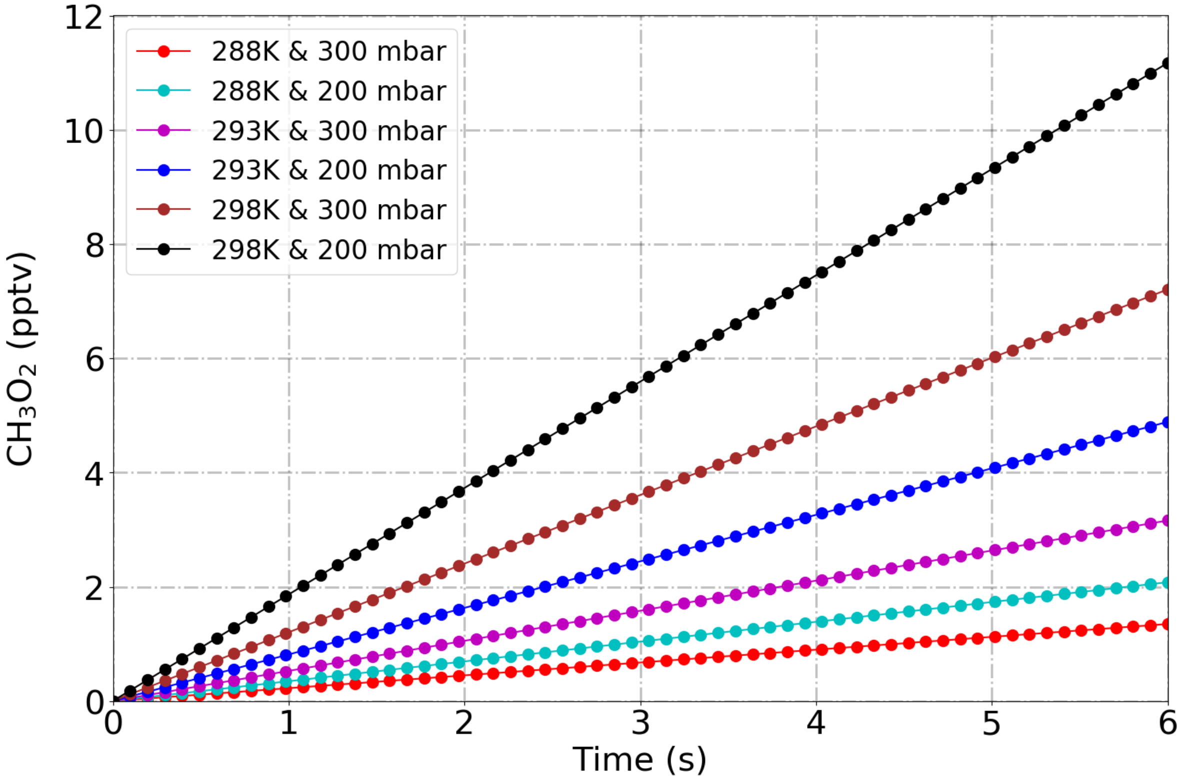

Figure 11: Box model simulation of the CH_3O_2 radical production from the thermal decomposition of 1 ppbv PAN at different temperatures and pressure.

625

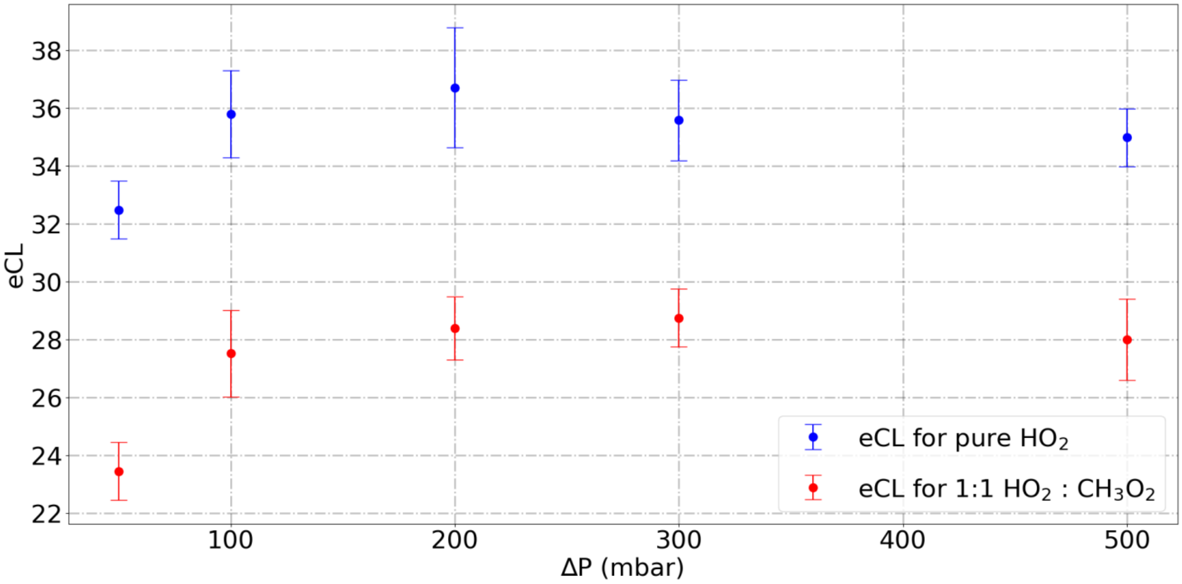

Figure 12: Dependency of eCL on ΔP (ΔP = $P_{ambient}$ - P_{inlet}) as determined for PeRCEAS under controlled laboratory conditions for 45 ppmv NO and 300 mbar inlet pressure. The error bars represent the 1σ deviation of identical calibrations at each ΔP.

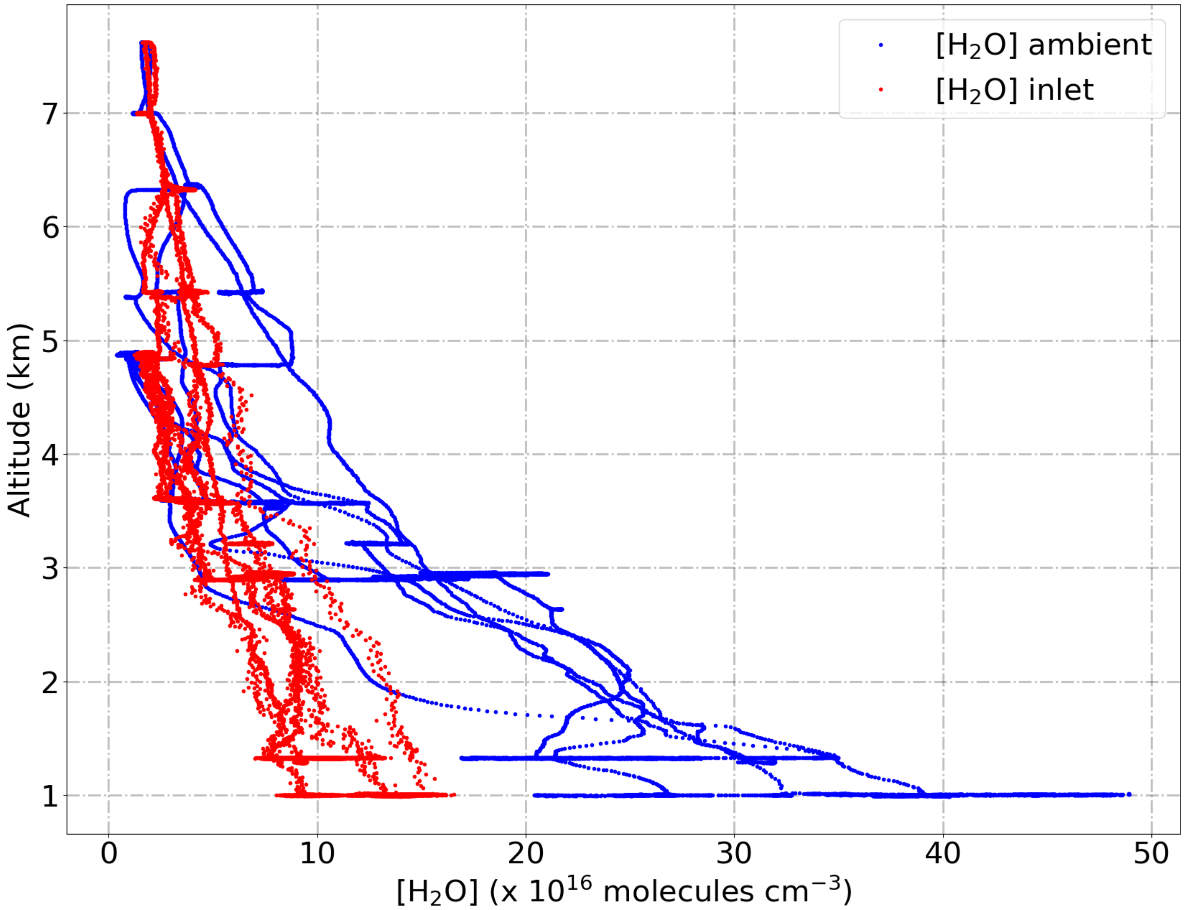

Figure 13: Example of vertical [H_2O] distribution measured by BAHAMAS on board HALO in July 2017 during the EMeRGe campaign in Europe. The humidity measured inside the DUALER is plotted in red for comparison.

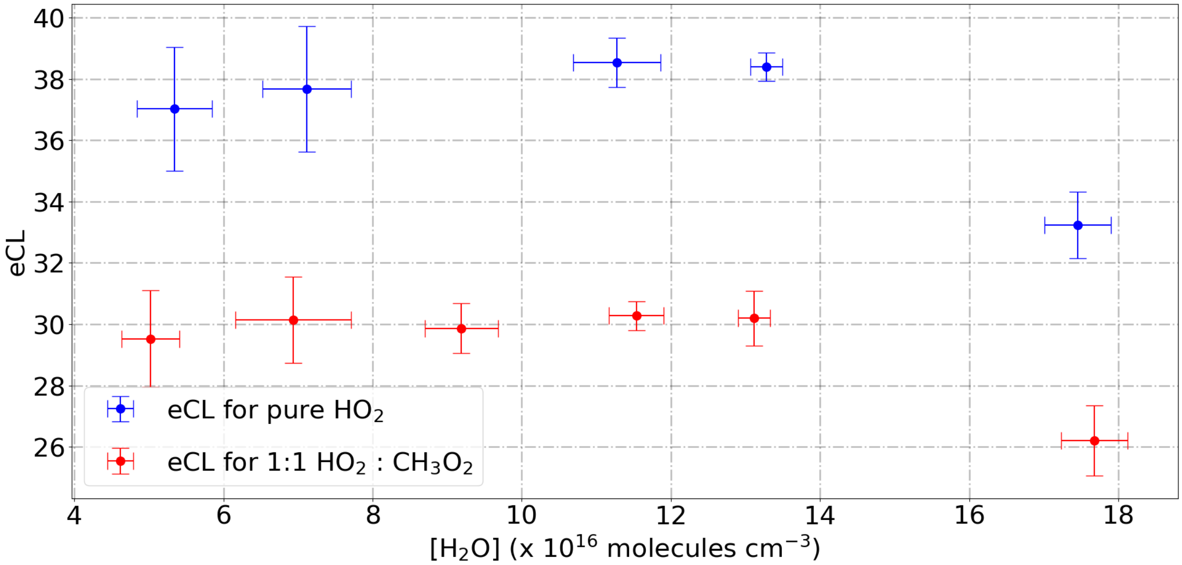

Figure 14: Dependency of PeRCEAS eCL on inlet humidity at constant sampling flow, inlet pressure, ΔP, [NO], [CO] and [N_2].

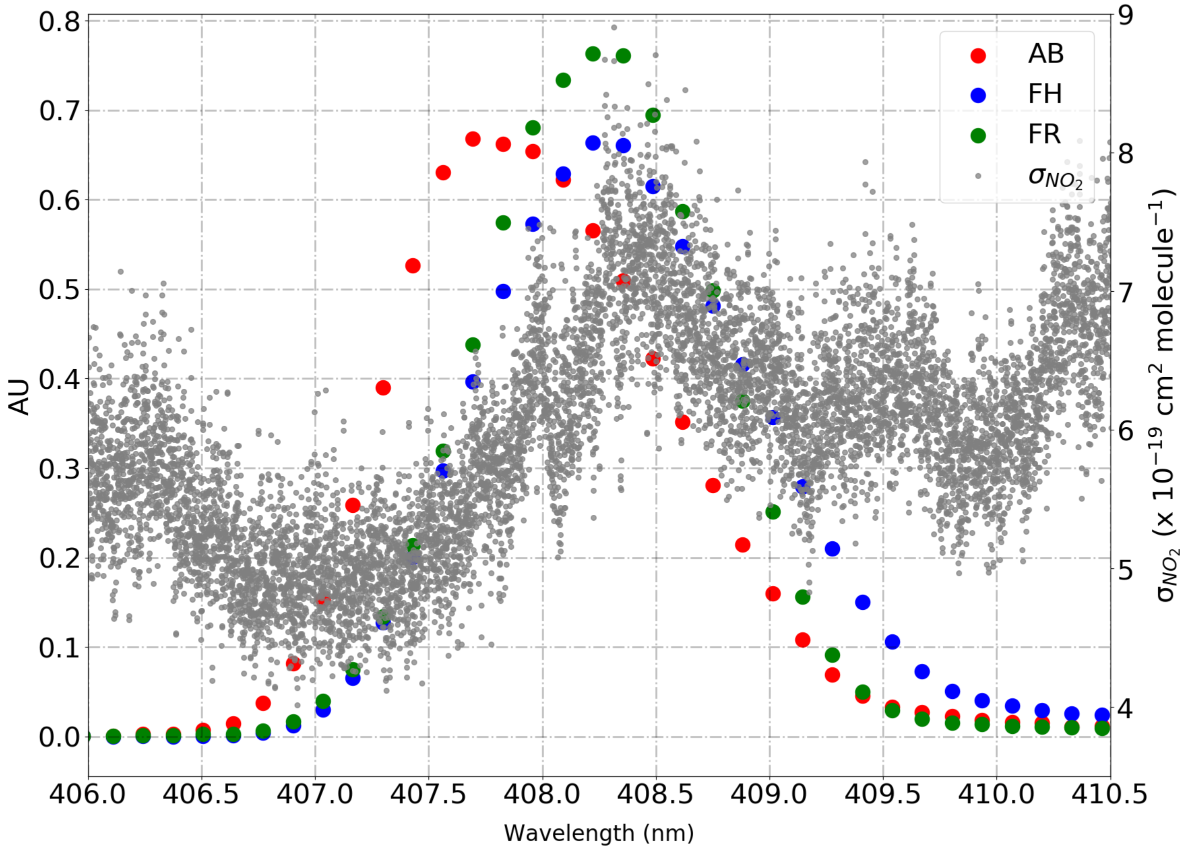

Figure 15: Emission spectrum of the lasers used by PeRCEAS. The high resolution σ_{NO_2} at 294 K from Vandaele et al (2002) is also depicted for comparison.

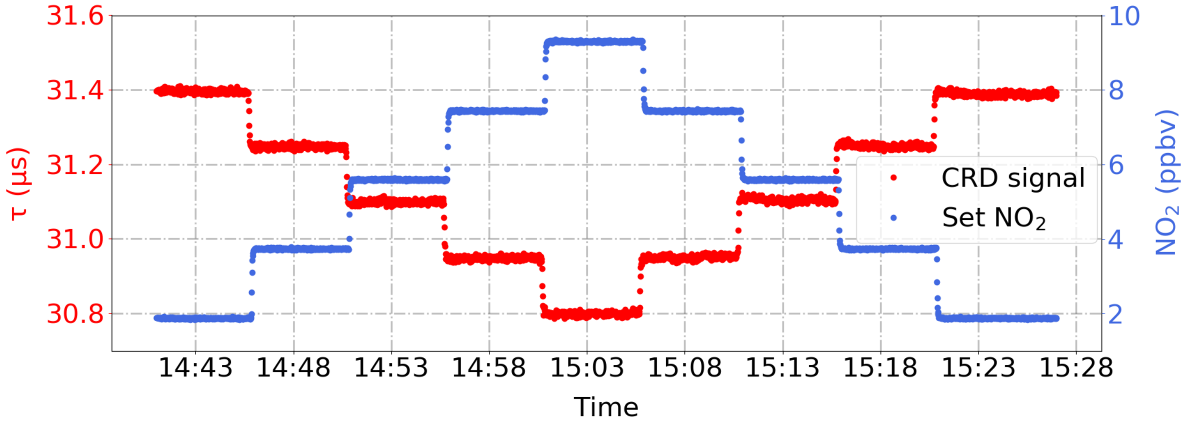

Figure 16: PeRCEAS measurement of known NO_2 mixing ratios in synthetic air (Airliquid 9.89 ± 0.2 ppmv NO_2 in SA) using the FH detector at 200 mbar and 500 ml/min sample flow.

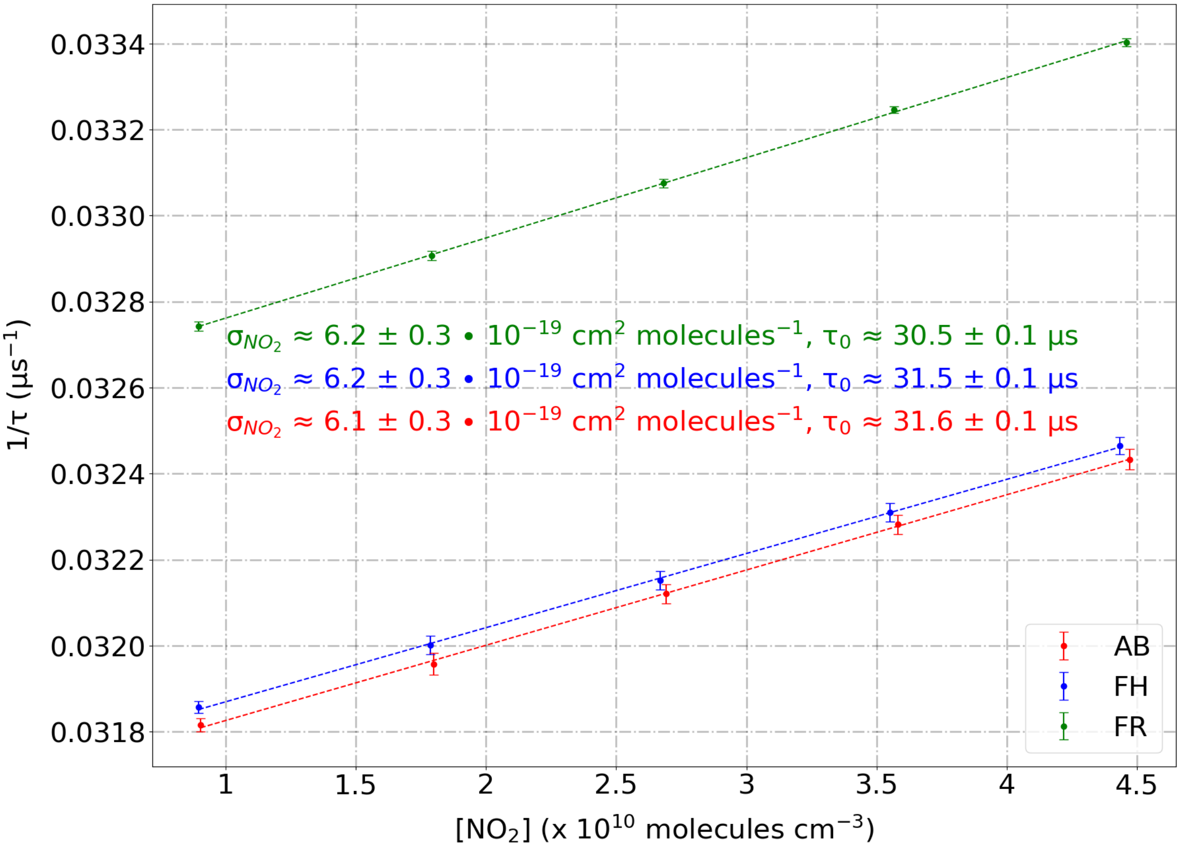

Figure 17: Effective absorption cross section, σ_{NO_2}, obtained from NO_2 calibrations carried out at 200 mbar detector pressure for the PeRCEAS detectors: AB (red), FH (blue) and FR (green). Linear fits are also depicted for clarification.

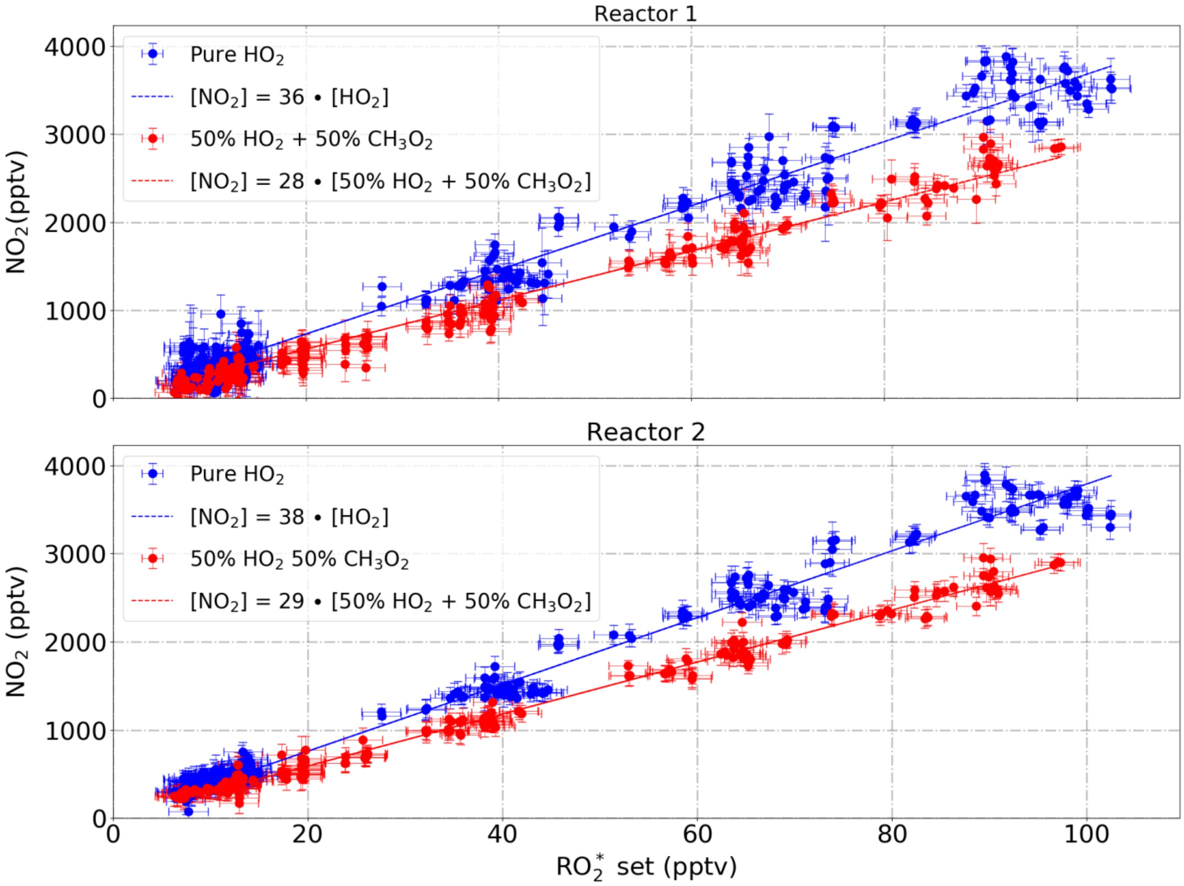

Figure 18: Experimental eCL determination of the DUALER II reactors from a series of 14 calibrations with generated mixing ratios of HO_2 (in blue) and a (1:1) HO_2: CH_3O_2 radical mixture (in red) at 300 mbar inlet pressure, 200 mbar ΔP and 45 ppmv added NO at the inlet.

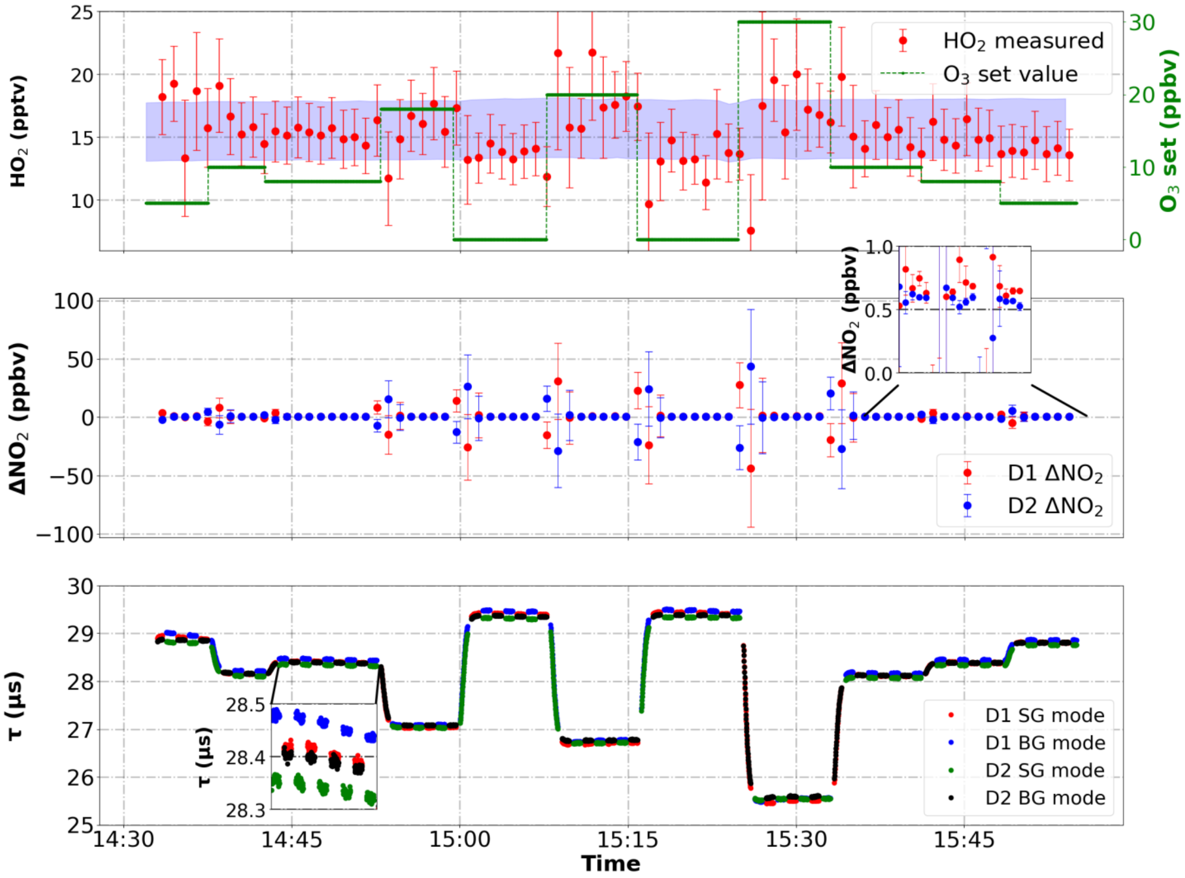

Figure 19: HO_2 retrieval while controlled changing O_3 background concentration under laboratory conditions using DUALER I. The blue shaded area shows the HO_2 produced in the source considering the 15 % uncertainty (2σ).

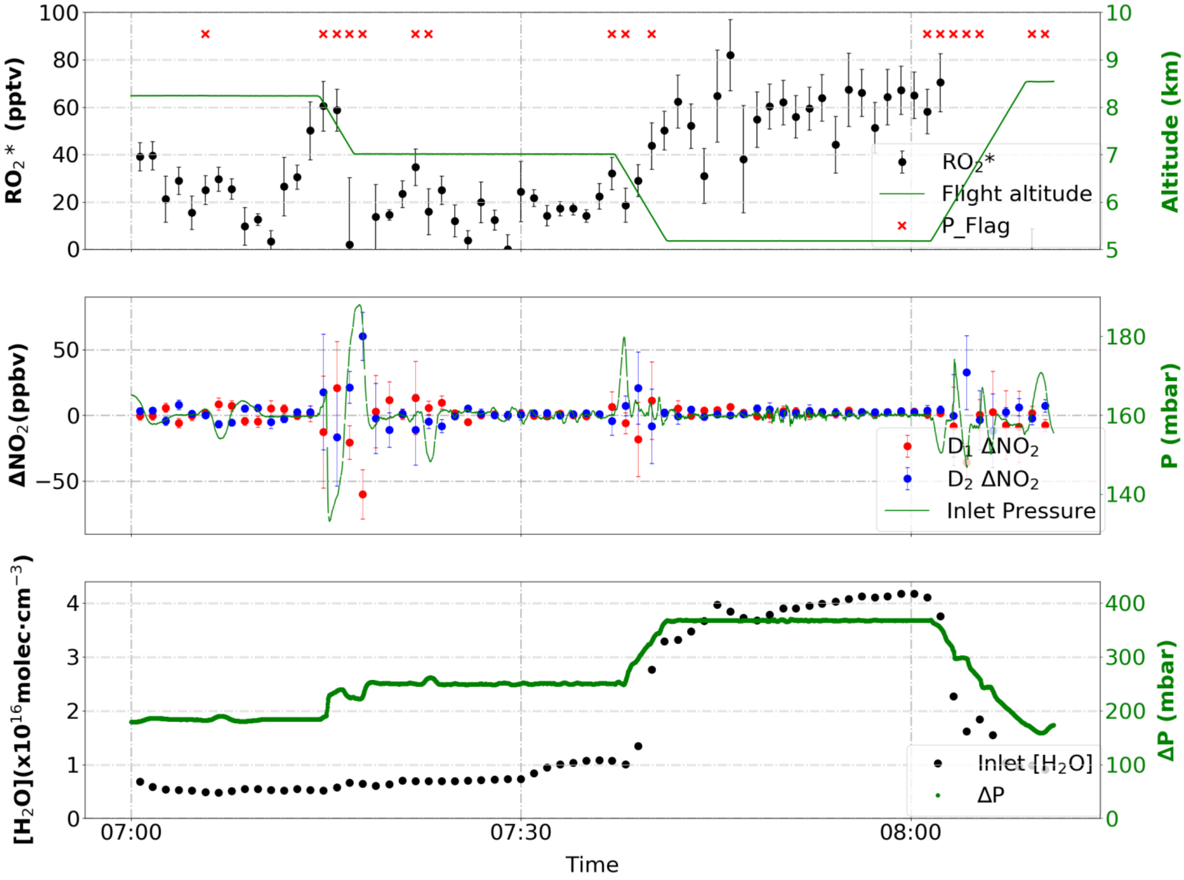

Figure 20: RO_2^* PeRCEAS airborne measurement during the OMO flight on 25.08.2015 at 160 mbar inlet pressure and with 15 ppmv NO added to the sample flow at the inlet.

https://doi.org/10.5194/amt-2019-359
Preprint. Discussion started: 14 October 2019

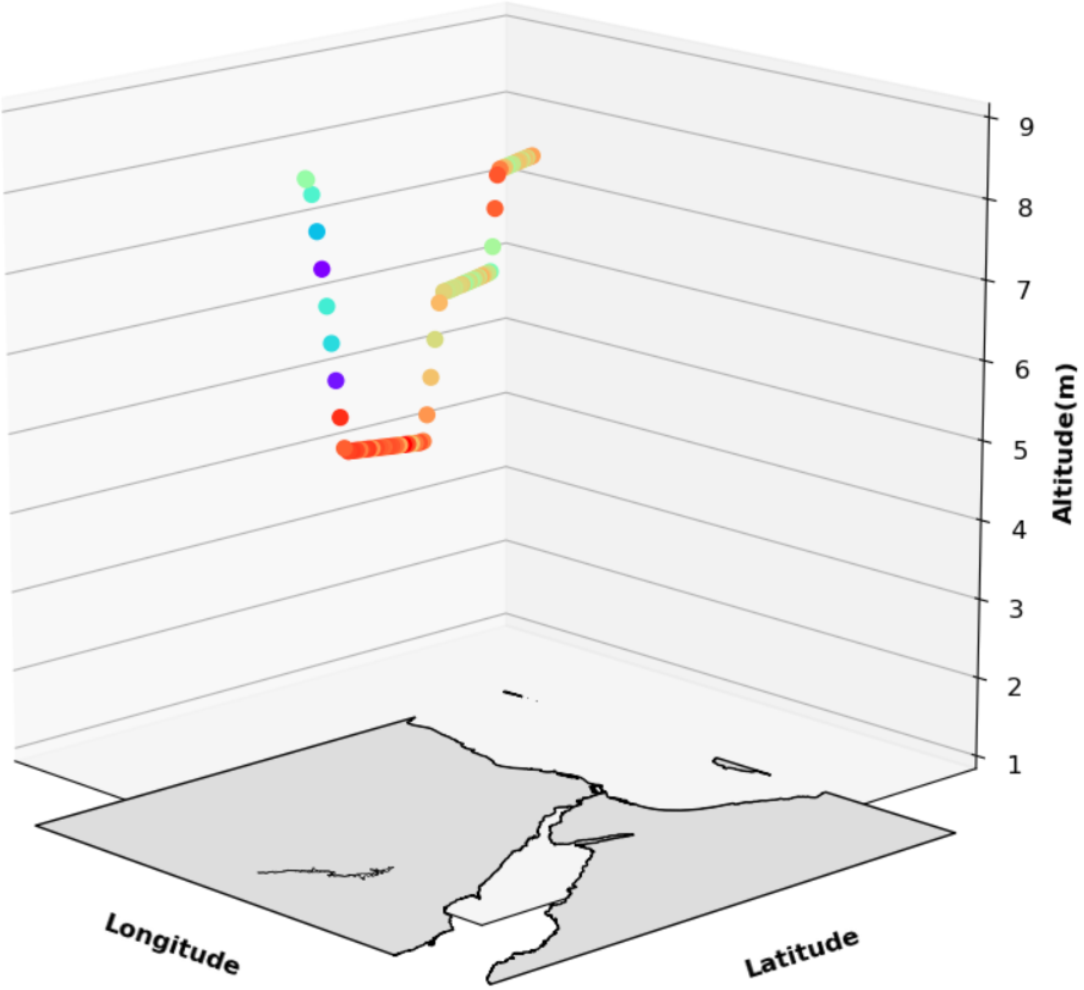

Figure 21: RO_2^* PeRCEAS measurements during the OMO flight on 25.08.2015 along the flight track.

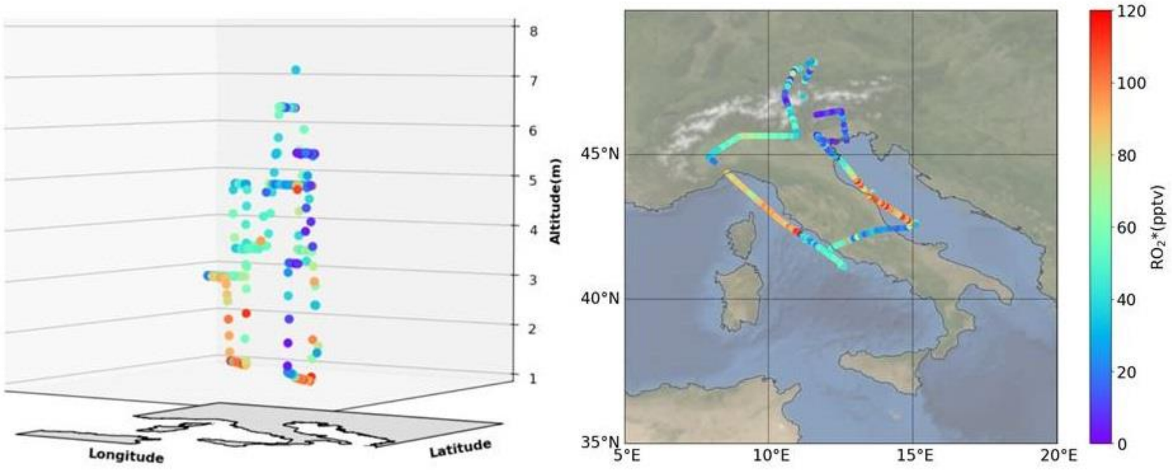

Figure 22: RO_2^* measurement along the flight track on 11.07.2017 during EMeRGe in Europe.

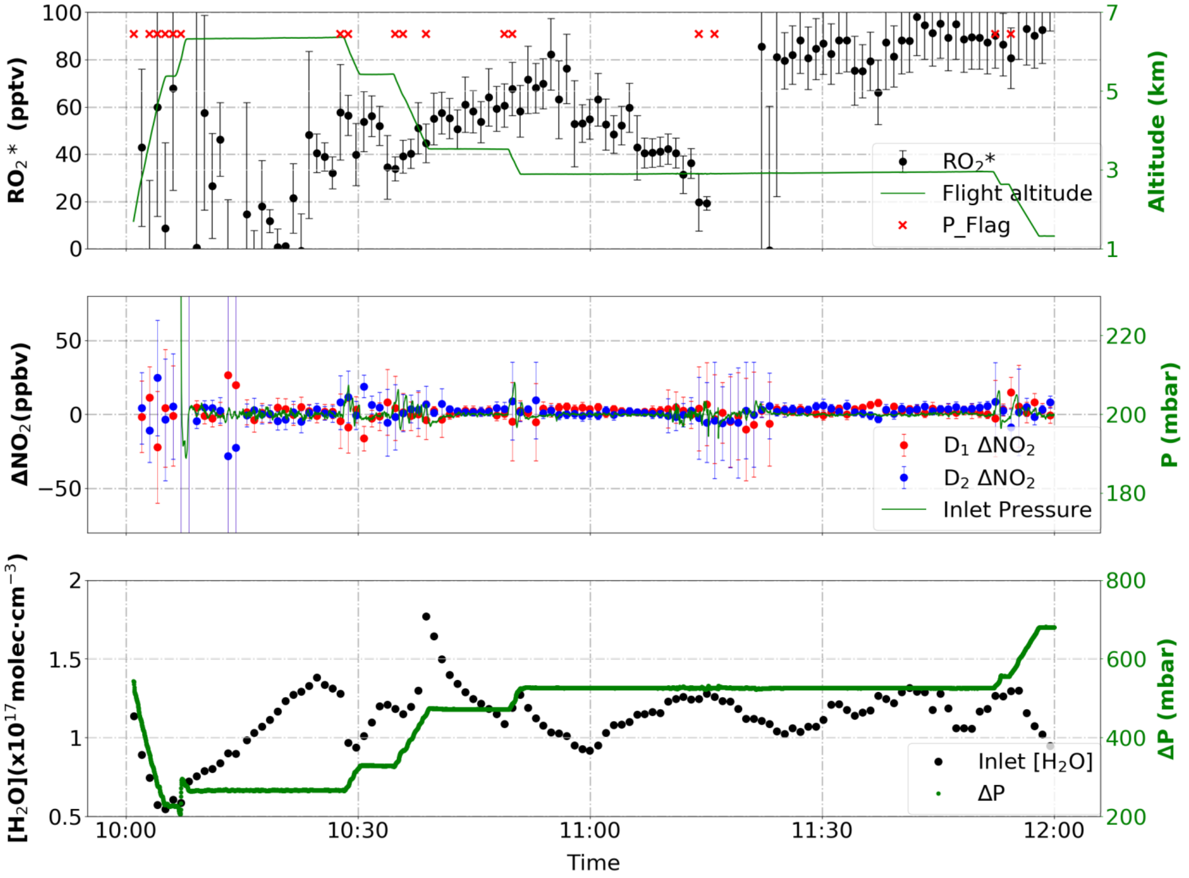

Figure 23: Detail of PeRCEAS airborne measurement during the EMeRGe flight on 11.07.2017 at 200 mbar inlet pressure and with 30 ppmv NO added to the sample flow at the inlet.